ELSEVIER

Thermochimica Acta 247 (1994) 129–168

thermochimica acta

Review

The caloric calibration of scanning calorimeters ☆

Stefan M. Sarge *, Eberhard Gmelin, Günther W.H. Höhne, Heiko K. Cammenga, Wolfgang Hemminger, Walter Eysel

(Recommendation of the working group "Calibration of Scanning Calorimeters" of the Gesellschaft für Thermische Analyse e.V. (GEFTA), Germany)

Received 19 July 1994; accepted 19 July 1994

Abstract

The present recommendation of the GEFTA working group "Calibration of Scanning Calorimeters" allows a precise heat and heat flow rate calibration of scanning calorimeters, largely independent of instrumental, sample-related and experimental parameters. Electric energy, electric power, heats of transition and heat capacities of suitable calibration substances are used for calibration. The measuring method, measuring and evaluation procedure, calibration materials, significant influencing factors, sources of error and detailed examples are presented for these calibration methods. Besides specific problems of heat measurement (interpolation of the baseline for the peak area determination) and heat capacity measurement (interpolation between initial and final isotherms, determination of the true heating rate of the sample, thermal lag of the sample), general aspects (thermodynamic fundamentals, difference between heat and heat flow rate calibration factor, weighing procedure) are also discussed.

Keywords: Calibration; Calorimeter; DSC; GEFTA

☆ Offprints can be obtained from the GEFTA office: Prof. Dr. V. Krämer, Kristallographisches Institut der Universität Freiburg, Hebelstraße 25, D-79104 Freiburg. A German version of this paper has been published in PTB-Mitteilungen 103 (1993) 49–512. The present publication contains revised data.

* Corresponding author at Physikalisch-Technische Bundesanstalt, Bundesallee 100, D-38116 Braunschweig, Germany.

SSDI 0040-6031(94)02015-9

Contents

1. Purpose and scope of the Recommendation 131

2. Documents to be taken into account 132

2.1. Recommendations for the nomenclature 132

2.2. Recommendations for temperature calibration 132

3. Definitions 132

4. Determination of relevant quantities from the curve of measured values 133

5. Calibration procedure 135

5.1. Heat flow rate calibration 136

5.1.1. Heat flow rate calibration by means of a known heat capacity 136
5.1.1.1. Calibration procedure 137
5.1.1.2. Systematic and statistical uncertainties 139

5.1.2. Heat flow rate calibration by means of electrical power 139
5.1.2.1. Calibration procedure 140
5.1.2.2. Systematic and statistical uncertainties 140

5.2. Heat calibration 141

5.2.1. Heat calibration by means of a known heat of transition 141
5.2.1.1. Calibration procedure 142
5.2.1.2. Systematic and statistical uncertainties 142

5.2.2. Heat calibration by means of electrical energy 143
5.2.2.1. Calibration procedure 143
5.2.2.2. Systematic and statistical uncertainties 143

6. Calibration substances 144

6.1. General requirements 144

6.2. Recommended calibration substances 145

6.3. Experimental conditions to be met 145

Annex 146

A1. Examples of caloric calibrations 146

A1.1. Heat flow rate calibration by means of electrical power 148

A1.2. Heat flow rate calibration by means of known heat capacities 150

A1.3. Heat calibration by means of electrical energy 154

A1.4. Heat calibration by means of known heats of transition 155

A2. Baseline interpolation for determination of the peak area 158

A3. Specific problems of heat capacity measurement 159

A3.1. Interpolation between the isothermal starting and end line for heat capacity determination 159

A3.2. Determination of the true sample heating rate 159

A3.3. Sample temperature lag 160

A4. Important thermodynamic fundamentals 161

A5. Difference between heat calibration factor and heat flow rate calibration factor 163

A6. Weighing regulation 164

A7. List of symbols 164

References 166

1. Purpose and scope of the Recommendation

The present Recommendation allows a correct caloric calibration of scanning calorimeters to be carried out independently of the instrumental parameters, up to a temperature of 1000 K. ("Scanning calorimetry" covers, among other things, differential scanning calorimetry (DSC).)

After reference to the relevant documents (Section 2), Section 3 gives the definitions of the terms which are important in caloric calibration, and Section 4 the rules according to which the relevant quantities (heat flow rate, heat) are determined. The calibration procedures are dealt with in Section 5, and suitable calibration substances are listed in Section 6. The Annex contains examples of calibrations and basic remarks on caloric calibration.

It is the purpose of this Recommendation to unify the methods used and thus eliminate error sources which would affect the reliability of calibration if other procedures were followed. As regards the caloric calibration of scanning calorimeters, particular mention must be made of the systematic difference between heat flow rate calibration and heat calibration (peak area calibration), the absolute amount of which is a function of the kind of measuring system used (see Annex A5). Because of this systematic difference, both the heat flow rate calibration (for the measurement of heat flow rates and heat capacities) and the heat calibration (to measure heats of transition and reaction) must be carried out. This also describes

the scope of this Recommendation: the precise caloric calibration of scanning calorimeters intended to measure heat flow rates/heat capacities and heats of transition/reaction.

2. Documents to be taken into account

2.1. Recommendations for the nomenclature [1,2]

John O. Hill (Ed.), For Better Thermal Analysis, 3rd edn., International Confederation for Thermal Analysis (ICTA), 1991, ISBN 0951762400 (may be obtained from Prof. P.K. Gallagher, Department of Chemistry, Ohio State University, 120 West 18th Avenue, Columbus, OH 43210-1173, USA).

Quantities, Units and Symbols in Physical Chemistry, 2nd edn., International Union of Pure and Applied Chemistry (IUPAC), Blackwell, Oxford, 1993, ISBN 0-632-03583-8.

2.2. Recommendations for temperature calibration [3,4]

G.W.H. Höhne, H.K. Cammenga, W. Eysel, E. Gmelin and W. Hemminger, Die Temperaturkalibrierung dynamischer Kalorimeter, PTB-Mitteilungen, 100 (1990) 25–31; The temperature calibration of scanning calorimeters, Thermochim. Acta, 160 (1990) 1–12.

H.K. Cammenga, W. Eysel, E. Gmelin, W. Hemminger, G.W.H. Höhne and S.M. Sarge, Die Temperaturkalibrierung dynamischer Kalorimeter II. Kalibriersubstanzen, PTB-Mitteilungen, 102 (1992) 13–18; The temperature calibration of scanning calorimeters. Part 2. Calibration substances, Thermochim. Acta, 219 (1993) 333–342.

3. Definitions

Caloric calibration comprises heat flow rate calibration and heat calibration (peak area calibration).

Heat flow rate calibration means the unique assignment of the heat flow rate measured by the calorimeter to the true heat flow rate taken up or released by the sample. The *measured heat flow rate* is proportional to a difference between the heat flow rate to the sample and the heat flow rate to the reference sample, which is in turn proportional to the temperature difference between sample and reference sample measuring system. The *displayed heat flow rate* also covers the *zero line heat flow rate* which occurs only as a result of asymmetries of the empty measuring systems (possibly with empty crucibles) (see below).

Heat flow rates taken up by the sample count as positive (endothermic), and heat flow rates released by the sample count as negative (exothermic). The symbol of the heat flow rate is Φ and the unit is the watt (W). As proportionality factor, heat flow

rate calibration determines the *calibration factor* K_Φ and its dependence on parameters (e.g. temperature); the calibration factor K_Φ links the measured heat flow rate Φ_m with the true sample heat flow rate Φ_{tr}

$$\Phi_{tr} = K_\Phi \Phi_m \tag{1}$$

The measured heat flow rate Φ_m is obtained from the displayed heat flow rate Φ_d and the zero line heat flow rate Φ_0

$$\Phi_m = \Phi_d - \Phi_0 \tag{2}$$

Heat calibration (peak area calibration) means the unique assignment of the heat measured by the calorimeter (peak area) to the true heat taken up or released by the sample as a result of transition (reaction).

The *measured heat* is assumed to be proportional to the area between the curve of measured values $\Phi_m(t)$, (t is time) and the interpolated baseline (see Annex A2) (*peak area*). In the following, a straight line between the peak onset, $\Phi_m(t_i)$, and the peak offset, $\Phi_m(t_f)$, is selected as the *interpolated baseline*.

Heat taken up by the sample is counted as positive (endothermic), and heat released by the sample to the environment is counted as negative (exothermic). The symbol of heat is Q; the unit is the joule (J). Heat calibration determines as the proportionality factor the *calibration factor* K_Q and its dependence on parameters (e.g. temperature); the calibration factor K_Q links the measured heat Q_m with the true sample heat Q_{tr}

$$Q_{tr} = K_Q Q_m \tag{3}$$

The calibration factors K_Φ and K_Q differ (see Annex A5).

4. Determination of relevant quantities from the curve of measured values

In an endothermic process (see Fig. 1), the calorimeter records a heat flow rate signal over the temperature. The curve of the values measured by the calorimeter with the crucibles empty is the *zero line*.

The terms required here, which are defined in the Recommendations for the Temperature Calibration of Scanning Calorimeters (see Section 2) are as follows: *peak*, curve section between T_i and T_f; *interpolated baseline*, here a straight line between T_i and T_f; *initial peak temperature*, T_i; *final peak temperature*, T_f.

Corresponding points of time are assigned to these characteristic temperatures (Fig. 1, initial peak time t_i and final peak time t_f). With the aid of the heating rate $\beta = dT/dt$, the relation between program temperature and time is obtained as

$$t = (T - T_{st})/\beta \Leftrightarrow T = T_{st} + \beta t \tag{4}$$

where T_{st} is the starting temperature. For the relation between sample temperature and program temperature see Annex A3.

The quantities necessary for heat flow rate calibration and heat calibration are defined in the following.

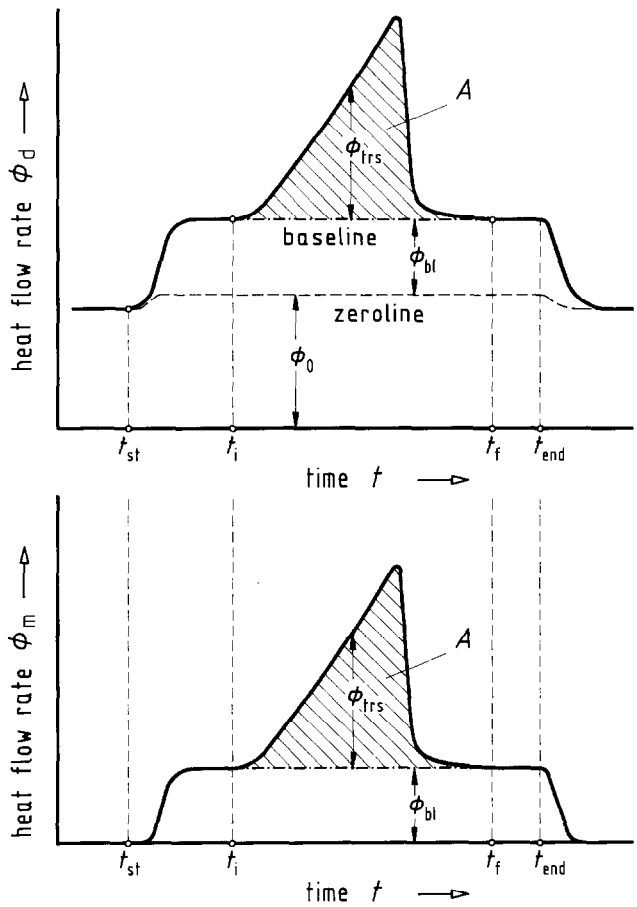

Fig. 1. Endothermic heat flow rate Φ_d displayed by a differential scanning calorimeter as a function of the time t (top). The heating program is started at the time t_{st} and switched off at the time t_{end}. The characteristic times t_i and t_f designate the peak onset and the peak offset. The interpolated baseline is a straight line in the peak area between $\Phi_d(t_i)$ and $\Phi_d(t_f)$. The zero line heat flow rate Φ_0 (separate measurement) is due to the thermal asymmetry of the differential measuring system, including the crucibles. In the stationary case, the baseline heat flow rate Φ_{bl} is proportional to the heat capacity of the sample and to the heating rate (empty reference sample crucible). The heat flow rate Φ_{trs} is due to the transition of the sample substance. The lower figure shows the measured heat flow rate Φ_m as the difference between the displayed overall heat flow rate Φ_d and the zero line heat flow rate Φ_0 determined by separate measurement. The peak area is the area A between the curve of measured values and the interpolated baseline (see also Annex A2).

In the case of transitions (see Fig. 1), the displayed heat flow rate Φ_d (with the reference sample crucible empty and crucibles of the same heat capacity) is composed of the zero line component Φ_0, the component for the sample heat capacity $\Phi_{bl} \propto C_S\beta$ and the component for the transition Φ_{trs}

$$\Phi_d = \Phi_0 + \Phi_{bl} + \Phi_{trs} = \Phi_0 + \Phi_m \tag{5}$$

The heat flow rate Φ_m flowing into the sample is obtained from the vertical spacing between the zero line and the curve $\Phi_d(t)$, Φ_{bl} from the spacing between the zero line and the interpolated baseline, and Φ_{trs} from the spacing between the interpolated baseline and the curve of measured values $\Phi_d(t)$ or $\Phi_m(t)$. The zero line heat flow rate Φ_0 is obtained from the spacing between the zero display of the calorimeter and the zero line. With modern scanning calorimeters, the ordinate value Φ_d is recorded in watts so that the calibration factor K_Φ is given without dimension (unit W/W).

The measured heat Q_m is represented by the peak area A (Fig. 1). For the correct determination of the heat of transition, reference is made to the relevant literature (see Annex A2).

In the peak area determination in general, the area determined with the aid of a straight line as the interpolated baseline is an approximation for the heat of transition. This linear baseline can be approximately assumed for the transitions of the pure substances (e.g. when indium is melted) proposed here for caloric calibration, because in these cases there are only slight differences between the heat capacity of the solid and liquid phase. Another prerequisite is that the conditions of heat transfer do not change during transition.

For the peak area A

$$A = \int_{t_i}^{t_f} [\Phi_m(t) - \Phi_{bl}(t)]\, dt = \int_{t_i}^{t_f} \Phi_{trs}(t)\, dt \tag{6}$$

In peak area calibration, the measured heat Q_m is taken directly as the peak area A

$$Q_{tr} = K_Q Q_m = K_Q A \tag{7}$$

As a product of heat flow rate and time, the peak area is in joules so that the calibration factor K_Q is given without dimension (J/J).

5. Calibration procedure

The calibration factors K_Φ and K_Q are functions of various parameters (e.g. temperature, heating rate, sample mass) (see Annex A5). Due to the complex (and generally unknown) dependence, the calibration procedure should basically be as similar to the measurement procedure as possible. Any dependence can be detected by two calibration measurements with the parameter in question being varied; this parameter is selected so that the effect of the subsequent measurement is included in the effect of the two calibration measurements. To detect nonlinear dependences, it is recommended that at least one calibration measurement be carried out in the interpolated interval. Special attention is drawn to the fact that K_Q and K_Φ are usually functions of the heating rate; the same heating rate must therefore be used for calibration and measurement.

The following effects have proved to be suitable for the calibration of scanning calorimeters: electrically generated heats and heat flow rates which can be directly measured with high accuracy; heats of phase transition and heat flow rates

which result when the temperature of a material of known heat capacity changes and which are indirectly realized with calibration substances.

The procedures described below are applicable both to heating and cooling. There are, however, restrictions for heat calibration by means of heats of transition in the cooling mode (see Section 5.2.1).

After the calorimeter has been calibrated for the whole temperature range, the validity of this calibration should be verified by regular selective checks. It is recommended that temperature calibration will have been carried out for the calorimeter by the method recommended by GEFTA (for references see Section 2) so that the corrected temperature corresponds to the true temperature in the isothermal state (for heat flow rate calibrations by means of a known heat capacity; see, however, Annex A3).

5.1. Heat flow rate calibration

5.1.1. Heat flow rate calibration by means of a known heat capacity

Under ideal conditions, the difference between the true heat flow rates into the sample ($\Phi_{S,tr}$) and into the reference sample ($\Phi_{R,tr}$) is given by the difference between the heat capacities (generally heat capacities at constant pressure C_p; also see Annex A4) of the sample C_S and the reference sample C_R multiplied by the true heating rates

$$\Delta\Phi_{tr} = \Phi_{S,tr} - \Phi_{R,tr} = C_S \frac{dT_S}{dt} - C_R \frac{dT_R}{dt} \stackrel{!}{=} (C_S - C_R)\beta \tag{8}$$

In practice, the true heating rates dT_S/dt and dT_R/dt are replaced by the average heating rate β determined experimentally (see Annex A3). The true heat flow rate difference $\Delta\Phi_{tr}$ is determined from two curves of measured values. The first curve is the result of a measurement with sample and reference sample (sample measurement, $\Phi_d = \Delta\Phi_{SR}$) and the second curve is obtained from a measurement with the crucibles empty (crucibles of the same mass as in the first measurement, zero line, $\Phi_d = \Phi_0$). The difference between the two curves of measured values, multiplied by the calibration factor, yields the true heat flow rate difference

$$\Delta\Phi_{tr} = K_\Phi(\Delta\Phi_{SR} - \Phi_0) \tag{9}$$

The zero line describes the asymmetry of the measuring system and of the crucibles used. The following is therefore valid for the calibration factor:

$$K_\Phi = \frac{(C_S - C_R)\beta}{\Delta\Phi_{SR} - \Phi_0} \tag{10}$$

To increase the symmetry of the arrangement, a reference sample with a heat capacity similar to that of the measurement sample can be used. Generally, however, the measurements are carried out with the reference sample crucible empty, i.e. $C_R = 0$ and $\Phi_d = \Phi_S$, so that

$$K_\Phi = \frac{C_S\beta}{\Phi_S - \Phi_0} \tag{11}$$

5.1.1.1. Calibration procedure. Every measurement consists of three steps which can also be identified in the curve of measured values (see Fig. 2). To determine the starting line $\Phi_{iso,st}$, the measuring system is first kept isothermal; subsequently, the temperature interval of interest is traversed up to the final temperature at the desired heating rate (generally 10 K min^{-1}). Then the end line $\Phi_{iso,end}$ is determined in the isothermal state. For the measurement with crucibles empty, Φ_0, and the calibration sample measurement, $\Phi_{S,cal}$, the same temperature program is used.

If the isothermal starting and end lines of calibration sample measurement and measurement with the crucibles empty are displaced in relation to one another, this will be corrected for by subtraction of two interpolated straight lines Φ_i (see Figs. 2 and 3). To obtain these, the heat flow rate value of the isothermal starting line at t_{st} and the heat flow rate value of the isothermal end line (extrapolated to t_{end}) are required. The transformation of $\Phi_d(t)$ into $\Phi'_d(t)$ (from Fig. 2 to Fig. 3) is performed according to the formula

$$\Phi'_d(t) = \Phi_d(t) - \left[\Phi_{iso,st} + \frac{\Phi_{iso,end} - \Phi_{iso,st}}{t_{end} - t_{st}}(t - t_{st})\right] \tag{12}$$

With the relationship $T = f(t)$ (which is usually nonlinear; see Annex A3), the following is valid for the calibration factor of heat flow rate measurements $K_\Phi(T)$:

$$K_\Phi(T) = \frac{C_{S,cal}(T)\beta}{\Phi'_{S,cal}(T) - \Phi'_0(T)} \tag{13}$$

For the calibration, the following procedure is to be followed:

(a) The calibration substance is to be selected in accordance with the requirements of Section 6.

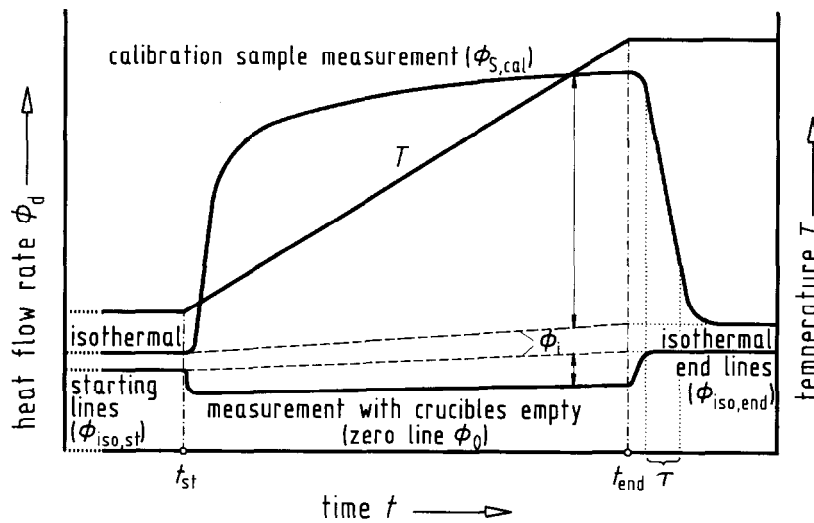

Fig. 2. Procedure for the heat flow rate calibration by means of known heat capacity.

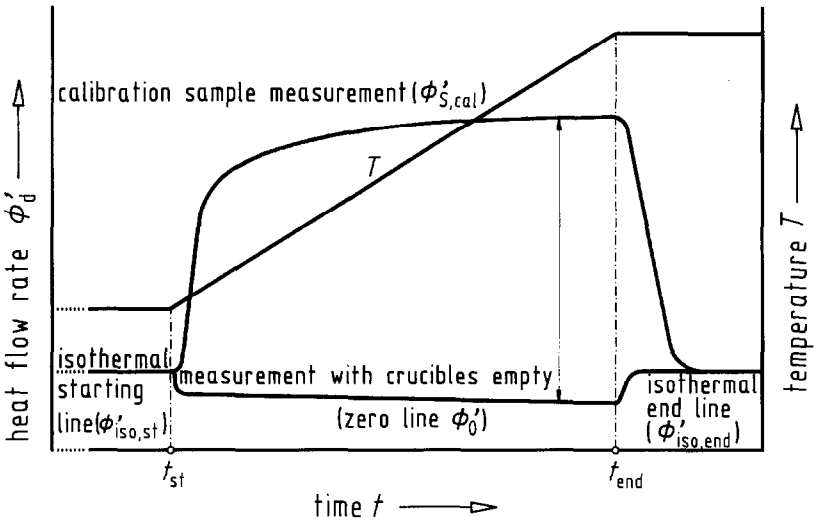

Fig. 3. Calculated heat flow rate Φ'_d after correction for the displacement of the isothermal starting and end lines (baseline and zero line).

(b) Measurements are to be carried out with at least two calibration samples of different heat capacity (mass); these are to be selected so that the heat capacity of the sample lies between the heat capacities of the calibration samples. Prior to each measurement of the calibration sample, a measurement with the crucibles empty is to be carried out. Each calibration sample measurement should be performed the same day as the associated measurements with the crucibles empty.

(c) Measurement samples and calibration samples are to be weighed into crucibles the shapes, sealings, emissivities and masses of which are as similar as possible or identical.

(d) Each of the three sections of the temperature program must last long enough to ensure quasi stationary conditions. This is the case after three to ten times the time constant τ (see Fig. 2) to be taken from the curve of measured values.

(e) Each measurement is to be repeated three times, and the same temperature program is to be used. The calibration sample measurements are to be carried out alternately with the associated measurements with the crucibles empty.

(f) In the quasi stationary range, related pairs of values obtained from measurements with the crucibles empty and calibration sample measurements are to be evaluated according to Eq. (13), and average values of $K_\Phi(T)$ are to be calculated for each sample. Differences in the mass (heat capacity differences) of the crucibles used for the measurements with the crucible empty and for the measurements of the calibration sample are to be taken into account by computation.

5.1.1.2. Systematic and statistical uncertainties. The overall uncertainty of calibration is basically composed of individual uncertainties, some of which can be

estimated only in terms of the order of magnitude. Attention is to be paid to the following points.

(1) The tabular values found in the literature and the fitting polynomials calculated from these values for the heat capacity of the calibration materials are affected by uncertainties.

(2) The weighings and reweighings (calibration sample crucible, empty crucible, calibration sample) are affected by uncertainties.

(3) The measurement of both the calibration sample and the empty crucibles (zero line) is affected by an uncertainty which results from the noise of the curve of measured values and the repeatability error.

(4) When the displacement of the isothermal starting and end line is allowed for, a linear temperature dependence of the displacement is assumed to a first approximation (see Annex A3).

(5) Particularly in the case of heat flow rate differential scanning calorimeters, the measured signal of heat flow rate is greatly dependent on the thermal coupling between sample and measuring system. The positioning of the sample in the crucible and of the crucible in the measuring system is therefore of particular importance for the magnitude of the repeatability error of the measurements.

(6) In the scanning mode, temperature gradients occur inside the sample and between sample and temperature sensor so that, (1) a mean sample heat capacity is measured over a temperature interval, (2) the temperature displayed by the calorimeter does not correspond to the mean sample temperature, and (3) the true sample heating rate is modified. The magnitude of these effects depends on the heating or cooling rate selected, on the heat capacity of the samples, the crucibles and the measuring system, and on the prevailing heat transfer conditions (see Annex A3).

(7) The selected evaluation limits, which are determined by the switch-on behaviour of the calorimeter, and the applied evaluation algorithms influence the result.

5.1.2. Heat flow rate calibration by means of electrical power

Heat flow rate calibration should be carried out by means of electrically generated heat flow rates if there is enough space for a heating resistor and its supply lines. With disc-type measuring systems, this is only exceptionally the case. For DSC devices with a cylindrical measuring system, calibration heaters are often commercially available.

For the amount of heat flow rate $|\Phi_{tr}|$ generated in an ohmic resistor R

$$|\Phi_{tr}| = UI \tag{14}$$

is valid. The voltage U and the current I can be determined with high accuracy and thus a potential temperature dependence of the heating resistor is also covered. The measured heat flow rate Φ_m is given by the difference between the displayed heat flow rate Φ_d, with the electric current switched on, and the zero line heat flow rate Φ_0 with the electric current switched off ($\Phi_m = \Phi_d - \Phi_0$). The calibration factor then is

$$K_\Phi = \frac{\Phi_{tr}}{\Phi_m} = \frac{UI}{|\Phi_m|} \tag{15}$$

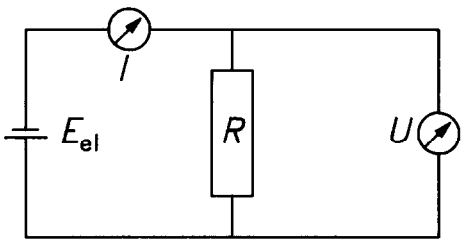

Fig. 4. Circuit diagram for determining the power in electric calibration. E_{el} is the power supply, U the voltage measurement, I the current measurement and R the calibration resistor.

5.1.2.1. Calibration procedure. For electrical calibration, a heating resistor must be installed in the calorimeter, in the place of the sample. Calibration heater and supply lines are to be selected such that the Joule heat in the calibration heater is maximal and the heat conduction to the environment minimal.

The heating power is determined by simultaneously measuring current and voltage using four wires. Two-wire measurement will be appropriate only if the temperature dependences $R(T)$ of both resistances and the ratio of the calibration resistance to the supply line resistance are known (see Fig. 4).

The calibration measurement is carried out by analogy with the procedure described in Section 5.1.1.1 (a) to (f); however, the following differences should be noted:

(i) In the place of the calibration substance, the calibration heater is used to realize a defined heat flow rate.

(ii) In place of calibration samples with different heat capacities, different heating powers are to be selected.

(iii) During the measurement, the calibration heat flow rate $|\Phi_{tr}| = UI$ is to be switched on and off several times. The separate determination of the zero line can thus be dispensed with, and a curve such as that shown in Fig. 5 is obtained.

5.1.2.2. Systematic and statistical uncertainties. The overall uncertainty of calibration is influenced by the following parameters:

(1) Uncertainty of measurement of the electrical quantities U and I.

(2) In the electric supply lines, the Joule heat $|\Phi_w| = I^2R_w$ is generated, which contributes to an unknown extent to the heating of the sample. Annex A1.3 (example of a calibration) describes how this error can be corrected.

(3) The electric supply lines constitute an additional heat leak which is difficult to determine and can vary with the measurement temperature. The overall leak of the measuring system is altered by the supply lines so that the transferability of the calibration result to the subsequent measurements becomes uncertain.

(4) The heat transfer resistances of calibration resistor and measurement sample to the measuring system are different and can give rise to systematic differences.

(5) As to further uncertainties, reference is made to Section 5.1.1.2, points (3) (noise and repeatability error of the curve of measured values), (5) (positioning of the calibration heater in the crucible and measuring system) and (7) (evaluation).

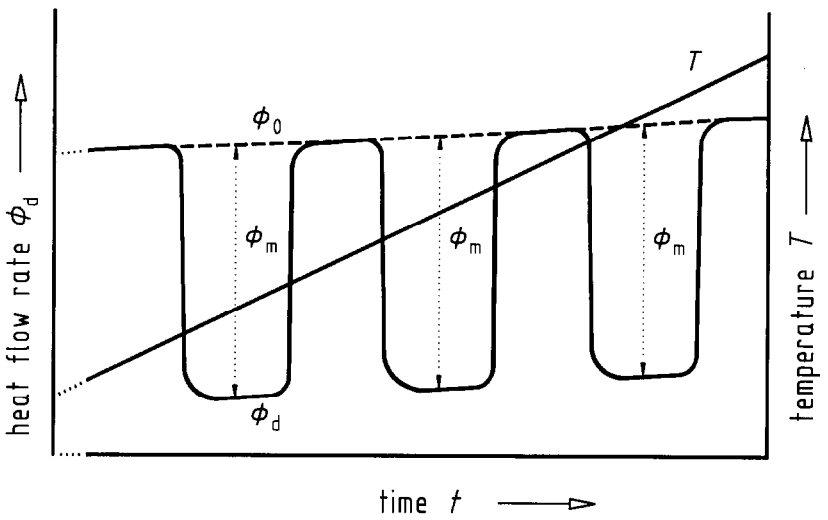

Fig. 5. Curve of measured values and interpolated baselines in heat flow rate calibration by means of electric power. See text for explanation.

5.2. Heat calibration

5.2.1. Heat calibration by means of a known heat of transition

Under ideal conditions, the true sample heat Q_{tr} is equal to the enthalpy difference $\Delta_{trs}H$ in the case of a first-order phase transition of the calibration substance. According to Fig. 1 and Eq. (7), the true sample heat Q_{tr} is linked with the measured peak area A.

According to Section 4, the following is therefore valid for the calibration factor K_Q at the temperature T_{trs} of the transition:

$$K_Q(T_{trs}) = \frac{Q_{tr}}{Q_m} = \frac{Q_{tr}}{A} = \frac{Q_{tr}}{\int_{t_i}^{t_f}[\Phi_m(t) - \Phi_{bl}(t)]\,dt} \stackrel{!}{=} \frac{\Delta_{trs}H}{\int_{t_i}^{t_f}[\Phi_m(t) - \Phi_{bl}(t)]\,dt} \qquad (16)$$

Note that in principle integration is to be made over the time and *not* over the temperature (see Annex A4).

In reality, the true heat of transition Q_{tr} can differ from the enthalpy of transition $\Delta_{trs}H$ (see Annex A4, Eq. (A9)). As a result of the temperature dependence of the enthalpy of transition (see Annex A4, Eq. (A13)), the heats of transition occurring in the cooling mode can differ from those occurring in the heating mode if there is large-scale undercooling.

5.2.1.1. Calibration procedure. The calibration is to be carried out as follows:

(a) The calibration substances are to be selected in accordance with the requirements of Section 6; their transition temperatures must cover the temperature range of interest in sufficient number.

(b) Measurements are to be carried out with at least two calibration samples having different heats of transition Q_{tr} (mass); the masses are to be selected so that the heat measured for the sample lies between the heats of transition of the calibration samples. The calibration samples should be measured the same day, if possible.

(c) Samples under investigation and calibration samples are to be weighed into crucibles, the shapes, sealings and emissivities of which are as similar as possible or identical.

(d) According to the heating rate selected (generally 5 K min^{-1}), the starting and end temperature of the calibration measurement must be selected such that the baseline between t_i and t_f (see Fig. 1) can be clearly interpolated. To achieve this, the scanning section of the temperature program must be long enough to ensure quasi stationary conditions both prior to and after phase transition.

(e) Each measurement is to be repeated three times, and the same temperature program is to be used. Each time the calibration sample and the crucible are to be removed from, and placed back into, the measuring system.

(f) The calibration factor $K_Q(T)$ is to be calculated for each measurement. For each sample (mass) the average value of K_Q is computed.

5.2.1.2. Systematic and statistical uncertainties. The overall uncertainty of heat calibration determined from a known heat of transition is composed of the following individual uncertainties:

(1) The values given in the literature for the enthalpy of transition are affected by uncertainties. In addition, the difference between the thermodynamically defined enthalpy of transition and the heat of transition determined in the scanning calorimeter is to be allowed for.

(2) The weighings and reweighings (calibration sample crucible, calibration sample) are affected by uncertainties.

(3) The noise of the curve of measured values and its repeatability error influence the determination of the peak area.

(4) The determination of the peak area is affected by an uncertainty which depends on the type of baseline construction (see Annex A2), the position of the integration limits (t_i and t_f in Fig. 1) and the evaluation algorithm.

(5) Particularly in the case of heat flow rate differential scanning calorimeters, the measured heat signal also depends on the thermal coupling between sample and measuring system. The positioning of the sample in the crucible and of the crucible in the measuring system is therefore of importance for the magnitude of the repeatability error of the measurements. It must be taken into account that after the first melting, due to the surface tension, metals generally form a sphere with a small contact area with the crucible bottom, whereas organic materials generally wet the crucible bottom after the first melting.

5.2.2. Heat calibration by means of electrical energy

Heat calibration should be carried out by means of electrically generated heat if there is enough space for a heating resistor and its supply lines. DSC devices with

a cylindrical measuring system can generally be easily calibrated with electrical energy using a calibration heater. With disc-type measuring systems, this is possible only in exceptional cases. The practical realization of a calibration heater is difficult; commercial devices are not available.

For the amount of the Joule heat $|Q_{tr}|$ released in an ohmic resistor

$$|Q_{tr}| = \int_{t_1}^{t_2} UI \, dt \tag{17}$$

is valid where U is the voltage, I the electric current and t the heating time, all of which can be determined with high accuracy. A potential temperature dependence of the heating resistor is then covered as well. According to Fig. 1 and Eq. (6), the measured heat Q_m is given by the area within the integration limits between the measured heat flow rate Φ_m with electric power and the baseline heat flow rate Φ_{bl} ($\Phi_m = \Phi_d - \Phi_0$). The calibration factor thus is

$$K_Q = \frac{Q_{tr}}{Q_m} = \frac{Q_{tr}}{|A|} = \frac{\int_{t_1}^{t_2} UI \, dt}{|A|} = \frac{\int_{t_1}^{t_2} UI \, dt}{\left|\int_{t_i}^{t_f} [\Phi_m(t) - \Phi_{bl}(t)] \, dt\right|} \tag{18}$$

5.2.2.1. Calibration procedure. To the installation of the calibration heater and the determination of the heating power, the specifications of Section 5.1.2.1 (paragraphs 1 and 2) apply. In addition, the heating time is to be determined.

The calibration measurement is carried out by analogy with the procedure described in Section 5.2.1.1 (a) to (f): however, the following differences should be noted:

(i) In the place of the calibration substances, the calibration heater is used here to realize defined heats.

(ii) In the place of calibration samples with different heats of transition, different heating powers are to be selected so that the shapes of the electrically generated heat pulses correspond more or less to the curve resulting from the phase transition of the sample measured; the peak area shall lie between the areas of the calibration peaks.

(iii) To determine the temperature dependence of the calibration factor, these heat pulses must be generated at different temperatures. A curve such as that shown in Fig. 6 results.

5.2.2.2. Systematic and statistical uncertainties. As regards the estimate of the overall uncertainty, the specifications of Section 5.1.2.2, points (1) (uncertainty of measurement of electrical quantities), (2) (Joule heat of the supply lines), (3) (heat leak through supply lines) and (4) (heat transfer resistances) as well as of Section 5.2.1.2 points (3) (noise and repeatability error of the curve of measured values) and (4) (peak area determination) are applicable to the electric heat calibration. The uncertainty of the determination of the heating time t must also be taken into consideration.

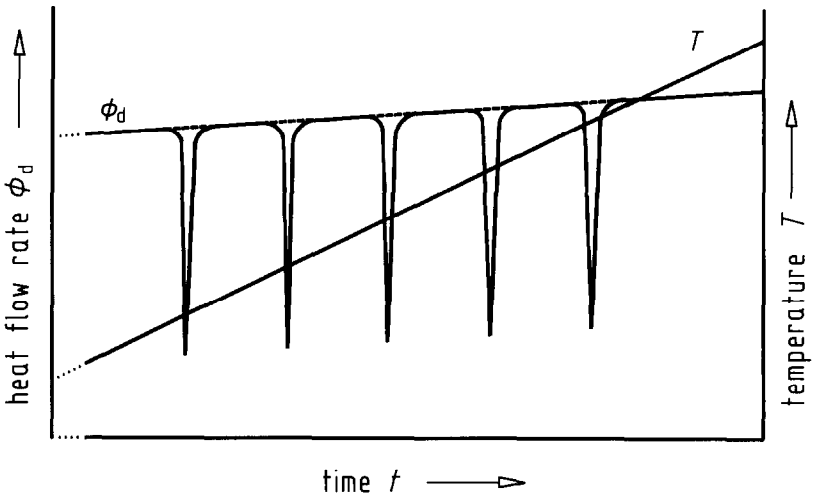

Fig. 6. Curve of measured values and interpolated baselines in heat calibration by means of electrical energy.

6. Calibration substances

6.1. General requirements

For reasons of economic efficiency, it should also be possible to use calibration substances intended for caloric calibration for temperature calibration. Other requirements are as follows:

(i) The heat capacity or the heat of transition should be known from measurements using two different adiabatic calorimeters, if possible.

(ii) The substance must be available with sufficient purity (no measurable influence of impurities on heat capacity or heat of transition).

(iii) Reactions with the crucible material and the ambient atmosphere and photoreactions must not occur.

(iv) The substance must be of long-term stability, non hygroscopic and of low volatility.

(v) The substance should be recognized as being physiologically safe.

For a substance for heat flow rate calibration, the following additional requirements are valid:

(i) In the temperature range applied, no transition must take place.

(ii) Reliable fitting polynomials must be available for the heat capacity values.

For a substance for heat calibration, the following additional requirements are valid:

(i) It must exhibit a defined first-order phase transition.

(ii) The variation of the heat capacity due to the phase transition should be small.

(iii) The transition should be without overheating phenomena (no influence of nucleation).

(iv) A reliable best value must be available for the heat of transition.

6.2. Recommended calibration substances

The calibration substances referred to in Tables 1–3 were selected with regard to the criteria mentioned. Many other substances recommended in the literature were checked but did not meet the requirements. For example, platinum has not been accepted as a substance for heat flow rate calibration, because the values of the heat capacity are not known with sufficient accuracy (requirement: uncertainty $\leq 0.5\%$; available for Pt: $\pm 1\%$). Zinc is another example which has not been accepted as a substance for heat calibration, because the peak area and shape vary when repeat measurements are carried out in an aluminium crucible.

6.3. Experimental conditions to be met

The requirements of Section 6.1 are to be complied with. Furthermore, the following factors are to be taken into account:

(i) For each calibration (consisting of several measurements), the calibration sample is to be weighed separately. When metals are used, any oxide layer is to be removed beforehand.

(ii) Only one grain (crystal, particle) should be used in order to avoid multiple peaks (heat calibration) and to allow the calibration value to be exactly assigned to the temperature (effect of the temperature gradient in the crucible).

Table 1
Substances for heat flow rate calibration

Substance	Temperature range in K	Polynomial [a] $C_p(T)$ in J g^{-1} K^{-1}	Uncertainty in %	Ref.	Remarks
Corundum (α-Al_2O_3)	70–300	$\sum_{i=0}^{7} a_i T^i$	0.4–0.1	[5]	NIST SRM 720 (synthetic sapphire) [b]
	290–2250	$\sum_{i=0}^{7} b_i T^i$	0.1–0.2		No limitation on crucible material below T_{fus}
Copper (Cu)	20 97.5	$\sum_{i=0}^{6} c_i T^i$	0.1	[6]	OFHC quality [c]
	97.5–320	$\sum_{i=0}^{4} d_i T^i$	0.1		No limitation on crucible material below T_{fus}

[a] At the limits of the respective temperature ranges, the polynomials given are also fitted with respect to the first derivative dC_p/dT. See Table 2 for values. [b] National Institute of Standards and Technology, USA, standard reference material. [c] Oxygen-free, high conductivity.

Table 2
Coefficients of the fitting polynomials for the heat capacity of the heat flow rate calibration materials

i	a	b	c	d
0	3.63245×10^{-02}	-5.81126×10^{-01}	1.43745×10^{-02}	-1.63570×10^{-01}
1	-1.11472×10^{-03}	8.25981×10^{-03}	-1.21086×10^{-03}	7.07745×10^{-03}
2	-5.38683×10^{-06}	-1.76767×10^{-05}	-1.23305×10^{-05}	-3.78932×10^{-05}
3	5.96137×10^{-07}	2.17663×10^{-08}	4.20514×10^{-06}	9.60753×10^{-08}
4	-4.92923×10^{-09}	-1.60541×10^{-11}	-8.49738×10^{-08}	-9.36151×10^{-11}
5	1.83001×10^{-11}	7.01732×10^{-15}	6.71459×10^{-10}	
6	-3.36754×10^{-14}	-1.67621×10^{-18}	-1.94071×10^{-12}	
7	2.50251×10^{-17}	1.68486×10^{-22}		

(iii) The position of the calibration sample in the crucible should agree with the position of the sample to be investigated and with the position of the sample used for temperature calibration (see above, temperature gradient in the crucible).

(iv) The furnace atmosphere, the gas pressure and the gas flow velocity and also the crucible must be the same during calibration and measurement.

(v) The samples for heat calibration should not be heated beyond the transition temperature more than absolutely necessary (≤ 10 K) to minimize reactions between crucible material and sample. Subsequently, the sample must immediately be cooled as rapidly as possible until retransition to the initial phase has been observed.

(vi) The samples for heat flow rate calibration should be used only in temperature ranges in which a transition is excluded.

As regards the compatibility of the calibration substances with different crucible materials, reference is made to the publications cited in Section 2.2 and Table 3. For bismuth, the following applies in addition:

(i) No solubility and influence on the heat of fusion is to be expected for corundum (Al_2O_3), boron nitride (BN), graphite (C), silicate glass, quartz glass (SiO_2), oxidized aluminium, iron (Fe), molybdenum (Mo), tantalum (Ta), or tungsten (W).

(ii) The liquefied material dissolves the crucible material, and a heat of fusion variation is to be expected for aluminium (Al), silver (Ag), gold (Au) and nickel (Ni).

(iii) The compatibility for stainless steel and platinum (Pt) is not known.

The substance is never to be heated to a temperature substantially higher than the melting temperature.

Annex

A1. Examples of caloric calibrations

By selecting different devices and calibration substances and a wide temperature range, the following calibration examples demonstrate the wide range of application of this Recommendation.

Table 3
Substances for heat calibration

Substance	Temperature of transition		Enthalpy of transition		Uncertainty (2σ)	Type of transition	Ref.	Remarks
	in K	in °C	in J g^{-1}	in kJ mol^{-1}	in %			
Cyclo-	122.38	−150.77	69.60	4.881	0.5	Solid–solid	[7]	Only in a hermetically sealed crucible
pentane	138.06	−135.09	4.91	0.345	1.1	Solid–solid	[7]	Weighing-in as liquid, reweighing
	179.72	−93.43	8.63	0.605	1.1	Solid–liquid	[7]	for mass determination (see Annex A6)
Gallium	302.9146	29.7646	79.88	5.569	0.9	Solid–liquid	[8,9]	Liquefied material reacts with Al; pay attention to the strong undercooling
Indium	429.7485	156.5985	28.62	3.286	0.4	Solid–liquid	[10–14]	
Tin	505.078	231.928	60.40	7.170	0.6	Solid–liquid	[13–16]	Liquefied material reacts with Al and Pt
Bismuth	544.55	271.40	53.83	11.25	3.9	Solid–liquid	[17–19]	Liquefied material reacts with Al
Lithium sulphate	851.43	578.28	228.1	25.07	4.6	Solid–solid	[20–26]	Anhydrate hygroscopic; weighing-in as $Li_2SiO_4 \cdot H_2O$. Dehydration from 110°C, violent agitation of the particles in the crucible during dehydration; high water vapour pressure (do not use hermetically sealed crucible). Reweighing (see Annex A6)
Aluminium	933.473	660.323	398.1	10.74	2.3	Solid–liquid	[27–29]	Liquefied material reacts violently with Pt

A1.1. Heat flow rate calibration by means of electrical power

A scanning calorimeter with cylindrical measuring system (Setaram C80) was calibrated between 100°C and 200°C by means of electrical power. For this purpose, the calibration heater supplied by the manufacturer of the calorimeter was used. This device displays the heat flow rate Φ_m as a function of the voltage U_Φ of the thermopile in microvolts. The calibration factor K of this device therefore has the unit W/V, i.e. ampere (A).

When the power is determined by the four-wire technique, the heating power of the supply wires heated by the electric current is not taken into account and must therefore be determined experimentally. With a constant current source, at constant temperature (153°C), six measurements were carried out at a current I_{cal} of between 1 and 10 mA. Each measurement consisted of three partial measurements, each at constant current (see Fig. A1). (a) The heating current was carried via the current supply lines ($U_{\Phi,2I+H}$); (b) the heating current was carried via the potential taps ($U_{\Phi,2U+H}$); (c) the heating current was carried via a current supply line and the parallel potential tap ($U_{\Phi,I+U}$). With these six measurements a correction factor f_L was determined which gives the ratio of the heat $P_H\Delta t$ (Δt is the heating time (here 3600 s)) produced in the calibration heater alone, to the heat $P_{2I+H}\Delta t$ generated in the calibration heater and in the effective portion of the supply lines (see Table A1 and Fig. A2)

$$f_L = \frac{P_H\Delta t}{P_{2I+H}\Delta t} = \frac{R_H}{2R_I + R_H} = \frac{\int U_{\Phi,2I+H}\,dt + \int U_{\Phi,2U+H}\,dt - \int 2U_{\Phi,I+U}\,dt}{\int U_{\Phi,2I+H}\,dt} \quad \text{(A1)}$$

From this, a mean value of $f_L = 0.9940$ with a standard deviation $\sigma_{n-1} = 0.0008$ (0.08%) was obtained for the correction factor f_L. In the following, this correction factor is assumed to be independent of temperature, heating rate and power.

The calibration measurements were carried out in accordance with Section 5.1.2.1 using a power-stabilized current source with powers of 0.1, 1 and 10 mW (see Fig. A3). The heating times and the times between two heating periods were 3600 s. The heating rate was 0.1 K min^{-1}. For the calibration factor, the following is valid:

$$K_\Phi = \frac{UI}{f_L(U_{\Phi,m} - U_{\Phi,bl})} \quad \text{(A2)}$$

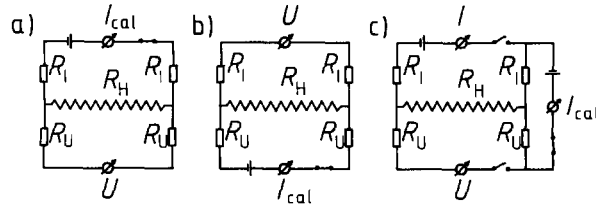

(a) $P_{2I+H} = 2P_I + P_H = (2R_I + R_H)I_{cal}^2$ Output signal $U_{\Phi,2I+H}$
(b) $P_{2U+H} = 2P_U + P_H = (2R_U + R_H)I_{cal}^2$ $U_{\Phi,2U+H}$
(c) $P_{I+U} = P_I + P_U = (R_I + R_U)I_{cal}^2$ $U_{\Phi,I+H}$

Fig. A1. Determination of the correction factor f_L to determine the Joule heat released in the supply wires.

Table A1
Effective power of the current supply lines

I_{cal} in mA	P in mW	$\sum U_{\Phi,2I+H}\,\Delta t$ in μV s	$\sum U_{\Phi,2U+H}\,\Delta t$ in μV s	$\sum U_{\Phi,I+U}\,\Delta t$ in μV s	f_L
1	1.000	101577	101532	441	0.99544
2	3.999	407138	406517	2535	0.99287
3	8.998	914085	914317	5614	0.99399
5	24.990	2538692	2538867	15666	0.99386
7	48.983	4976410	4976510	30620	0.99386
10	99.955	10152200	10152200	62436	0.99385

Table A2
Statistical data of the heat flow rate calibration curves determined through electrical calibration [a]

P in mW	s^2 in A^2	B
0.1	0.13643	0.91484
1	0.00787	0.99291
10	0.00004	0.99996
0.1; 1; 10	0.05680	0.95466

[a] P, electrical calibration power; s^2, variance; B, coefficient of regression.

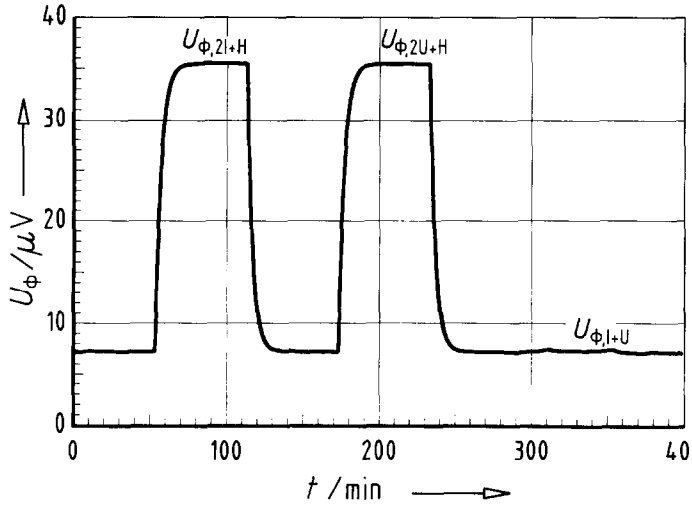

Fig. A2. Electrically generated calibration peaks to determine the heating power of the supply wires (correction factor f_L).

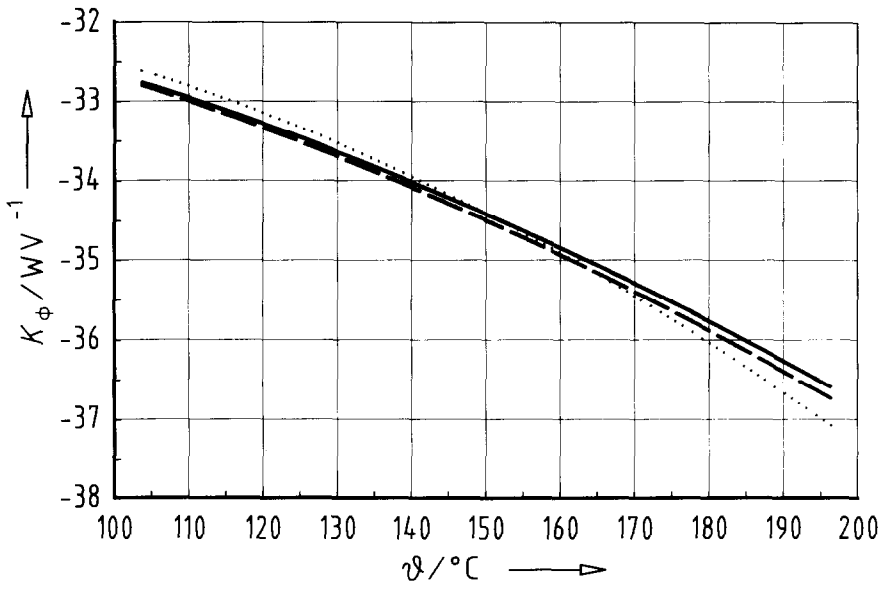

Fig. A3. Heat flow rate calibration curves determined through electrically generated heat flow rates. · · ·, $P = 0.1$ mW; – – –, $P = 1$ mW; ——, $P = 10$ mW.

The baseline $U_{\Phi,bl}$ was determined by first calculating a square function by regression over the last third of each currentless period; this function described the curvature of the zero line of the device. From the last thirds of the two baselines which included the respective heating peak, a linear function was subsequently calculated by regression. The calibration factor for the last third of the heating peak was obtained from Eq. (A2). The calibration factors thus determined can be described by a square function. Fig. A3 shows the calibration curves for each heating power applied, and Table A2 the statistical data of the regression curves determined.

The poor adaptation of the fitting parabola at the calibration power of $P = 0.1$ mW and the apparent power dependence can be attributed to the small signal-to-noise ratio ($S/N \approx 20$) and the uncertainty resulting when the baseline is determined by interpolation; a joint calibration curve independent of the power is therefore obtained as a result of heat flow rate calibration (see Table A2).

A1.2. Heat flow rate calibration by means of known heat capacities

A scanning calorimeter with disc-type measuring system (Du Pont 1090) was calibrated in the temperature range 100–300°C using corundum. To demonstrate the mass dependence, two sapphire single crystal discs of significantly different masses (129.60 and 7.79 mg) were placed in aluminium crucibles with lock-seamed covers. When these crucibles and two empty crucibles were selected, care was taken to ensure they were of equal mass (20.60 ± 0.03 mg).

These samples were subjected to the procedure described in Section 5.1.1.1. The temperature program was 5 min at 100°C, heating rate 10 K min^{-1}, 5 min at 300°C, All 12 measurements were performed on the same day. This device outputs the results in the form of graphs (see Fig. A4), the sign of the heat flow rate being opposite to the thermodynamic definition given here (see Section 3). For this device, the sample temperature in the quasi stationary range of the scanning phase (after 2–3 min) can be set equal to the program temperature. The maximum difference is 1 K (see Annex A3).

The measured heat capacities were determined as follows (see Table A3): At different times (corresponding to the two isotherms and selected program temperatures), a ruler was placed parallel to the ordinate, and the values for the curve of measured values (x_S) and the zero line (x_0) were read. Subsequently, the respective spacing Δx between the two curves was calculated. From the spacing between the isothermal starting lines and end lines, the correction Δx_{iso} for the respective times was determined; a linear relation between Δx_{iso} and the time has been assumed in the scanning range (5 to 25 min or 100 to 300°C). When this value is subtracted from Δx, $\Delta x'$ is obtained in millimetres; from this the differential heat flow rate (Fig. 3) is calculated with the aid of a scale factor f (f in mW mm^{-1}). From this,

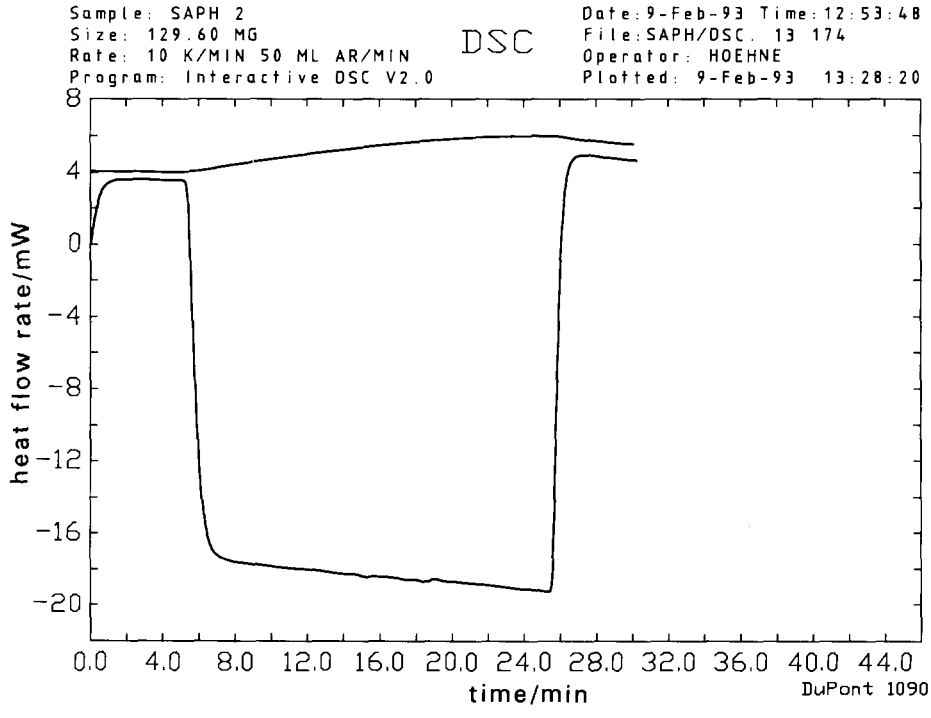

Fig. A4. Calibration sample measurement (lower curve) and associated measurement with the crucibles empty (upper curve) to determine the heat flow rate calibration factor by means of the known heat capacity of corundum.

Table A3
Results of a heat flow rate calibration by means of the known heat capacity of corundum

	Conditions							
	0–5 [a] Isothermal	7 [a] 120 [b]	9 [a] 140 [b]	13 [a] 180 [b]	17 [a] 220 [b]	21 [a] 260 [b]	25 [a] 300 [b]	25–30 [a] Isothermal
1st measurement (m = 129.60 mg)								
x_S/mm	22.9	143.2	164.4	167.2	151.1	150.0	150.4	14.0
x_0/mm	20.0	34.4	52.1	50.2	30.0	26.1	24.1	10.0
Δx/mm	2.9	108.8	112.3	117.0	121.1	123.9	126.3	4.0
Δx_{iso}/mm	2.9	3.0	3.1	3.3	3.6	3.8	4.0	4.0
$\Delta x'$/mm	0	105.8	109.2	113.7	117.5	120.1	122.3	0
c_m/J g^{-1} K^{-1}		0.9796	1.0111	1.0528	1.0880	1.1120	1.1324	
2nd measurement (m = 129.60 mg)								
x_S/mm	85.0	170.8	172.7	176.7	160.5	162.4	160.6	94.5
x_0/mm	82.5	63.0	61.3	60.8	40.3	39.6	35.0	90.0
Δx/mm	2.5	107.8	111.4	116.5	120.2	122.8	125.6	4.5
Δx_{iso}/mm	2.5	2.7	2.9	3.3	3.7	4.1	4.5	4.5
$\Delta x'$/mm	0	105.1	108.5	113.2	116.5	118.7	121.1	0
c_m/J g^{-1} K^{-1}		0.9730	1.0046	1.0481	1.0787	1.0991	1.1213	
3rd measurement (m = 129.60 mg)								
x_S/mm	55.0	184.2	168.0	173.7	173.5	171.8	169.5	83.5
x_0/mm	47.5	71.3	51.2	52.2	48.1	43.9	39.2	75.0
Δx/mm	7.5	112.9	116.8	121.5	125.4	127.9	130.3	8.5
Δx_{iso}/mm	7.5	7.6	7.7	7.9	8.1	8.3	8.5	8.5
$\Delta x'$/mm	0	105.3	109.1	113.6	117.3	119.6	121.8	0
c_m/J g^{-1} K^{-1}		0.9750	1.0102	1.0519	1.0861	1.1074	1.1278	
$\bar{c}_m$/J g^{-1} K^{-1}		0.9759	1.0086	1.0509	1.0843	1.1062	1.1272	
σ_{n-1}/J g^{-1} K^{-1}		0.003	0.004	0.002	0.005	0.007	0.006	
c_{tr}/J g^{-1} K^{-1}		0.9330	0.9577	1.0006	1.0360	1.0653	1.0899	
K_Φ(m = 129.60 mg)		0.956	0.950	0.952	0.955	0.963	0.967	

1st measurement ($m = 7.79$ mg)								
x_S/mm	60.0	143.8	153.6	163.9	171.8	181.3	178.3	81.2
x_0/mm	52.3	109.2	118.0	126.8	133.5	142.2	138.7	71.8
Δx/mm	7.7	34.6	35.6	37.1	38.3	39.1	39.6	9.4
Δx_{iso}/mm	7.7	7.9	8.0	8.3	8.7	9.1	9.4	9.4
$\Delta x'$/mm	0	26.7	27.6	28.8	29.6	30.0	30.2	0
c_m/J g^{-1} K^{-1}		1.0282	1.0629	1.1091	1.1399	1.1553	1.1630	
2nd measurement ($m = 7.79$ mg)								
x_S/mm	46.1	118.1	126.1	138.5	150.8	157.9	157.3	67.2
x_0/mm	40.0	84.7	92.0	103.0	113.9	120.4	119.0	60.0
Δx/mm	6.1	33.4	34.1	35.5	36.9	37.5	38.3	7.2
Δx_{iso}/mm	6.1	6.2	6.3	6.5	6.8	7.0	7.2	7.2
$\Delta x'$/mm	0	27.2	27.8	29.0	30.1	30.5	31.1	0
c_m/J g^{-1} K^{-1}		1.0475	1.0706	1.1168	1.1592	1.1746	1.1977	
3rd measurement ($m = 7.79$ mg)								
x_S/mm	46.2	153.0	146.0	145.0	150.0	150.0	145.0	54.9
x_0/mm	42.0	122.6	114.7	112.4	116.2	115.8	110.3	50.0
Δx/mm	4.2	30.4	31.3	32.6	33.8	34.2	34.7	4.9
Δx_{iso}/mm	4.2	4.3	4.3	4.5	4.6	4.8	4.9	4.9
$\Delta x'$/mm	0	26.1	27.0	28.1	29.2	29.4	29.8	0
c_m/J g^{-1} K^{-1}		1.0051	1.0398	1.0822	1.1245	1.1322	1.1476	
$\bar{c}_m$/J g^{-1} K^{-1}		1.0269	1.0578	1.1027	1.1412	1.1540	1.1694	
σ_{n-1}/J g^{-1} K^{-1}		0.021	0.016	0.018	0.017	0.021	0.025	
c_{tr}/J g^{-1} K^{-1}		0.9330	0.9577	1.0006	1.0360	1.0653	1.0899	
$K_\Phi(m = 7.79$ mg)		0.909	0.905	0.907	0.908	0.923	0.932	

[a] Time in minutes. [b] Program temperature in °C.

the measured heat capacity was determined as

$$c_m = \frac{\Delta x' f}{\beta m} \tag{A3}$$

The results of each group of three measurements were averaged and compared with those calculated for corundum according to Table 1. The calibration factor is calculated as

$$K_\Phi = \frac{c_{tr}}{c_m} \tag{A4}$$

The resulting calibration factors are represented in Fig. A5; in the calculation of the regression curve, the values at 120°C have not been taken into account, because the measuring system apparently had not yet reached the quasi stationary state. The calibration factors K_Φ differ significantly for the two masses; they differ also from the value $K_Q = 0.993$ which has been determined from the melting peak of indium.

A1.3. Heat calibration by means of electrical energy

A scanning calorimeter with cylindrical measuring system (Setaram C80) was calibrated between 100°C and 200°C by means of electrical energy. The calibration heater supplied by the manufacturer of the calorimeter was used for this purpose.

The calibration measurements were carried out with a power-stabilized current source with energies E_{el} of 0.03, 0.3 and 3 J ($P = 0.1$, 1, 10 mW). The heating time

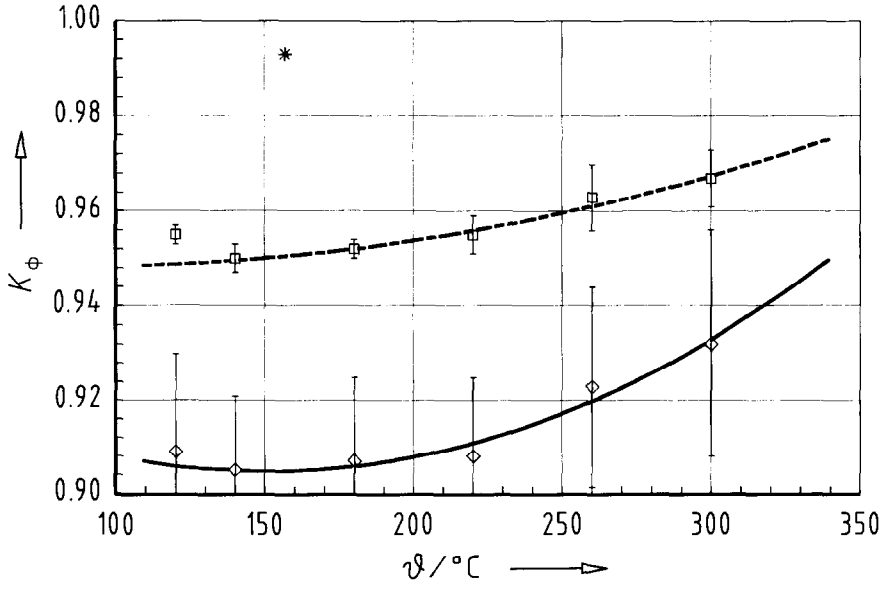

Fig. A5. Heat flow rate calibration factor from corundum measurements. —◇—, sample mass 7.79 mg; – – □ – –, sample mass 129.60 mg; ∗, heat calibration factor from indium measurement.

was in each case 300 s and thus of the same order of magnitude as the time constant of the device (approx. 220 s) so that peaks such as those recorded in the melting of a pure substance were obtained, although with opposite sign. The heating rate was 0.1 K min^{-1}. For the calibration factor the following is valid using the supply line correction factor f_L (see Annex A1.1)

$$K_Q = \frac{\int UI \, dt}{f_L \int (U_{\Phi,m} - U_{\Phi,bl}) \, dt} \tag{A5}$$

The baseline was determined by analogy with the procedure described in Annex A1.1. Table A4 and Fig. A6 show the results; in the determination of the regression curves, the values at 104°C were not taken into account. The statistical data of the regression curves determined are given in Table A5. Here again the poor correlation obtained when the heating energy of 0.03 J is used is attributable to the small signal-to-noise ratio ($S/N \approx 15$) and the resulting uncertainty of the baseline determination. In the range investigated, a significant dependence of the calibration factor on the applied electrical energy is not given for this device.

A1.4. Heat calibration by means of known heats of transition

A power-compensated scanning calorimeter (Perkin-Elmer DSC-2) was calibrated in the temperature range 120–310 K using calibration substances. For this purpose, three cyclopentane samples and three gallium samples were weighed into hermetically sealable aluminium crucibles (1.5–5 mg). These samples were sub-

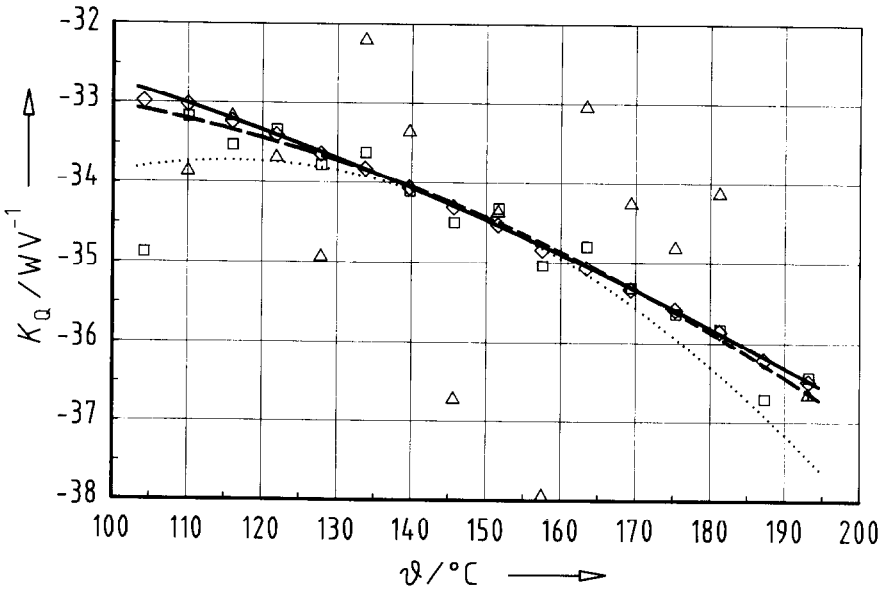

Fig. A6. Heat calibration functions determined by electrically generated heating energies E_{el}. Symbols give mean values; lines give regression parabolas. —— and ◇, $E_{el} = 3$ J; – – – and □, $E_{el} = 0.3$ J; · · · and △, $E_{el} = 0.03$ J.

Table A4
Heat calibration factors determined by electrical calibration

E_{el} in J	1st measurement		2nd measurement		3rd measurement		Mean values	
	θ in °C	K_Q in W V^{-1}	θ in °C	K_Q in W V^{-1}	θ in °C	K_Q in W V^{-1}	$\bar{\theta}$ in °C	$\bar{K}_Q$ in W V^{-1}
0.03	104.17	−42.51	104.17	−55.09	104.15	−55.68	104.16	−51.09
	110.09	−33.02	110.08	−37.48	110.07	−31.06	110.08	−33.85
	116.02	−30.83	116.02	−35.58	116.00	−33.11	116.02	−33.17
	121.94	−32.53	121.95	−35.23	121.95	−33.27	121.95	−33.68
	127.88	−37.74	127.88	−30.90	127.90	−36.15	127.89	−34.93
	133.79	−31.79	133.80	−32.36	133.81	−32.46	133.80	−32.20
	139.72	−33.54	139.74	−33.23	139.76	−33.29	139.74	−33.35
	145.66	−35.66	145.67	−38.38	145.71	−36.11	145.68	−36.72
	151.60	−34.52	151.61	−34.91	151.64	−33.66	151.61	−34.36
	157.52	−37.24	157.51	−38.60	157.56	−37.98	157.53	−37.94
	163.46	−35.48	163.45	−28.67	163.49	−34.96	163.47	−33.04
	169.40	−32.26	169.39	−34.66	169.43	−35.83	169.41	−34.25
	175.33	−36.03	175.33	−32.81	175.36	−35.57	175.34	−34.80
	181.27	−35.93	181.27	−32.24	181.31	−34.19	181.28	−34.12
	187.23	−42.05	171.24	−40.87	187.26	−39.94	187.24	−40.95
	193.15	−36.49	193.15	−35.37	193.19	−38.08	193.16	−36.65
0.30	104.36	−34.99	104.17	−34.77	104.19	−34.84	104.24	−34.87
	110.28	−33.03	110.10	−33.30	110.10	−33.18	110.16	−33.17
	116.21	−33.51	116.04	−33.60	116.04	−33.45	116.10	−33.52
	122.15	−33.27	121.96	−33.42	121.97	−33.29	122.03	−33.33
	128.08	−33.88	127.90	−33.76	127.90	−33.68	127.96	−33.77
	134.01	−33.64	133.82	−33.53	133.83	−33.67	133.89	−33.61
	139.95	−34.09	139.75	−34.25	139.77	−33.97	139.82	−34.10
	145.88	−34.46	145.70	−34.64	145.72	−34.37	145.77	−34.49
	151.83	−34.11	151.64	−34.39	151.63	−34.43	151.70	−34.31
	157.74	−35.29	157.56	−34.90	157.57	−34.92	157.62	−35.03
	163.67	−34.75	163.49	−34.87	163.49	−34.71	153.55	−34.78
	169.62	−35.35	169.44	−35.21	169.43	−35.37	169.31	−35.31
	175.55	−35.60	175.37	−35.73	175.36	−35.58	175.43	−35.63
	181.49	−35.85	181.32	−35.96	181.31	−35.65	181.37	−35.82
	187.46	−36.80	187.27	−36.75	187.26	−36.54	187.33	−36.70
	193.38	−36.54	193.20	−36.33	193.19	−36.40	193.25	−36.42
3.00	104.18	−32.99	104.18	−33.02	104.18	−32.94	104.18	−32.98
	110.10	−32.99	110.10	−33.03	110.10	−33.04	110.10	−33.02
	116.03	−33.22	116.03	−33.26	116.03	−33.21	116.03	−33.23
	121.96	−33.38	121.96	−33.45	121.96	−33.37	121.96	−33.40
	127.89	−33.61	127.89	−33.66	127.89	−33.61	127.89	−33.63
	133.81	−33.83	133.80	−33.81	133.81	−33.82	133.81	−33.82
	139.75	−34.00	139.73	−34.05	139.73	−34.11	139.74	−34.06
	145.71	−34.30	145.67	−34.29	145.68	−34.31	145.69	−34.30
	151.63	−34.52	151.60	−34.53	151.60	−34.51	151.61	−34.52
	157.55	−34.82	157.54	−34.84	157.54	−34.83	157.55	−34.83
	163.48	−35.06	163.47	−35.04	163.48	−35.08	163.48	−35.06
	169.42	−35.34	169.41	−35.33	169.42	−35.33	169.42	−35.33
	175.36	−35.58	175.35	−35.58	175.35	−35.59	175.35	−35.58
	181.30	−35.86	181.29	−35.88	181.29	−35.82	181.29	−35.85
	187.26	−36.21	187.25	−36.23	187.26	−36.20	187.26	−36.21
	193.18	−36.46	193.17	−36.49	193.16	−36.49	193.17	−36.48

Table A5
Statistical data for heat calibration curves determined by electrical calibration [a]

E_{el} in J	s^2 in A^2	B
0.03	4.1942	0.3035
0.3	0.0492	0.9668
3	0.0004	0.9997
0.03; 0.3; 3	2.1294	0.3722

[a] E_{el} is the electric calibration energy, s^2 the variance and B the coefficient of regression.

jected to the procedure described in Section 5.2.1.1. The heating rate was 5 K min^{-1}. For cyclopentane, the three transitions (see Table 2) were measured without the sample being removed. All 27 measurements were performed on the same day. Subsequently, the crucibles with cyclopentane were weighed again; after a small

Table A6
Results of the heat calibration by means of known heats of transition

Q_{tr} in J g^{-1}	Cyclopentane			Gallium
	ΔH(122 K) = 69.60 J g^{-1}	ΔH(138 K) = 4.91 J g^{-1}	ΔH(180 K) = 8.63 J g^{-1}	ΔH(303 K) = 79.88 J g^{-1}
1st sample	(m = 3.549 mg)			(m = 2.503 mg)
Q_m/J g^{-1}	72.818	4.944	8.594	83.02
	72.032	4.945	8.594	82.673
	72.029	4.921	8.624	82.604
$\bar{Q}_m$/J g^{-1}	72.29	4.937	8.604	82.77
σ_{n-1}/J g^{-1}	0.45	0.014	0.017	0.22
K_Q	0.963	0.995	1.003	0.965
σ_{n-1}	0.007	0.003	0.002	0.003
2nd sample	(m = 1.722 mg)			(m = 2.857 mg)
Q_m/J g^{-1}	72.731	4.954	8.147	81.902
	72.484	4.973	8.181	83.414
	72.025	4.966	8.301	83.539
$\bar{Q}_m$/J g^{-1}	72.41	4.964	(8.210) [a]	82.95
σ_{n-1}/J g^{-1}	0.36	0.010	0.081	0.91
K_Q	0.961	0.989	(1.051) [a]	0.963
σ_{n-1}	0.005	0.002	0.009	0.011
3rd sample	(m = 2.127 mg)			(m = 2.846 mg)
Q_m/J g^{-1}	71.734	4.859	8.688	81.283
	71.877	5.107	8.857	82.181
	72.061	4.936	8.754	82.042
$\bar{Q}_m$/J g^{-1}	71.89	4.967	8.766	81.84
σ_{n-1}/J g^{-1}	0.16	0.127	0.085	0.48
K_Q	0.968	0.988	0.984	0.976
σ_{n-1}	0.002	0.026	0.010	0.006

[a] Value not included in the evaluation.

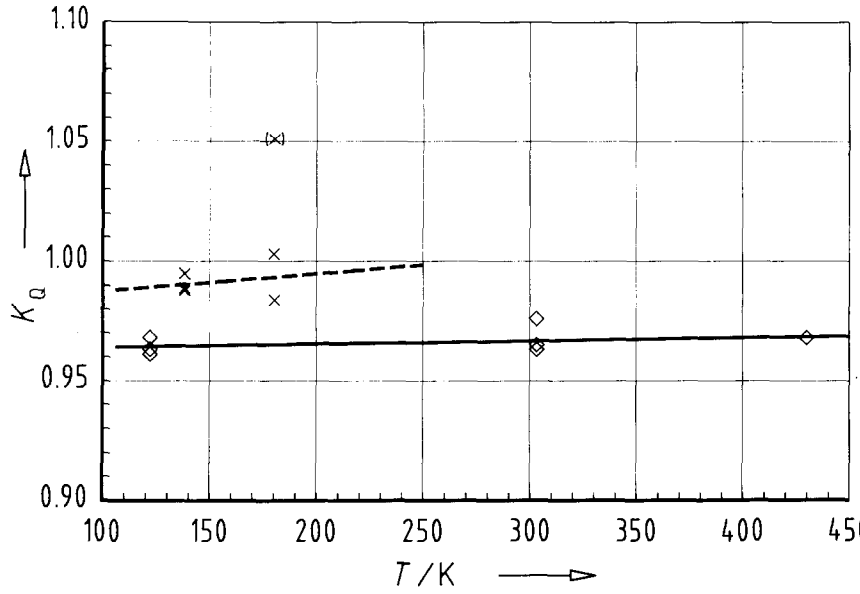

Fig. A7. Heat calibration factor for the lower temperature range: ——, calibration materials cyclopentane (solid–solid transition at 122 K), gallium (303 K) and indium (430 K); – – –, calibration material cyclopentane (solid–solid transition at 138 K, solid–liquid transition at 180 K). The point in brackets is considered to be an outlier and has not been included in the evaluation.

hole had been pierced, the cyclopentane was evaporated and the now empty crucibles were reweighed. The heats of transition (peak areas) were determined from the curves of measured values using a computer program. The results are given in Table A6. The calibration factors K_Q calculated according to Eq. (16) were averaged for each sample and are represented in Fig. A7.

When the value measured for indium at 430 K (i.e. $K_Q = 0.968$) (which has not been included in the table) is added, a calibration factor which is almost independent of the temperature is obtained (see Fig. A7, continuous line). The significant deviation for the transitions of cyclopentane at 138 K and 180 K (Fig. A7, broken line) shows the considerable dependence of the calibration factor on the thermal effect itself, because these transitions are accompanied by heats of transition which are smaller than those of the other transitions by a factor of approximately 10. Values in brackets were considered to be outliers and have not been included in the evaluation.

A2. Baseline interpolation for determination of the peak area

First-order phase transitions (without kinetic influence) are isothermal and generate a pulsed signal in the heat capacity/temperature function. However, due to the finite thermal conductivity, a scanning calorimeter always furnishes fairly broad

peak. For the accurate determination of the peak area, the interpolated baseline $\Phi_{bl}(t)$ and the integration limits t_i and t_f are required (see Fig. 1).

It is not possible to gain access to the baseline below the peak by experiment; its shape depends on the variation of the heat capacity and on the thermal coupling of the sample during transition. Variations of the heat capacity can be determined by computation and, if necessary, eliminated. Variations of the thermal coupling, however, lead to an uncertainty of the baseline determination.

Various methods have been proposed to take the influence of the heat capacity variation on the baseline into account [30]. The calibration substances recommended here show only a slight temperature dependence of the heat capacity in the solid and in the liquid state, a small variation of the heat capacity when melted and a negligible influence of the variation of thermal coupling; a straight line as a baseline is therefore a sufficiently good approximation to the "true" baseline, and it is not critical to fix the integration limits. In other cases, it is suitable from the thermodynamic point of view to determine the heat of the phase transition from the difference between the enthalpy curves extrapolated to the transition temperature. The enthalpy curves are obtained by integration of the heat capacity curves [31].

A3. Specific problems of heat capacity measurement

A3.1. Interpolation between the isothermal starting and end line for heat capacity determination

The procedure outlined in Section 5.1.1.1 for determining calibration factors for the determination of heat capacities is applicable only if the course of the interpolated isothermal baseline in the measurement of the calibration sample is identical with that of the interpolated isothermal zero line in the measurement with the crucibles empty. These curves are greatly dependent on the ambient temperature, the ambient atmosphere and the emissivity of the materials used. As the true shape of the curve can be neither measured nor controlled during the measurement, a measurement over a major temperature or time range is, if necessary, to be subdivided into partial measurements, because then interpolation must be carried out only over a small temperature range. In the borderline case, this leads to the accurate but time-consuming Isothermal Step Method [32]. If it is intended to measure continuously over a major temperature range, additional abscissae for the construction of the interpolated isothermal lines can be obtained by controlled cooling and insertion of intermediate isotherms [33].

A3.2. Determination of the true sample heating rate

Because the measured heat flow rate Φ_m of a scanning calorimeter is proportional to the heat capacity of the sample and its heating rate, the magnitude and the variations of the heating rate influence the uncertainty by which the determination of heat capacities is affected. A distinction is to be made between (i) the heating rate of the control thermometer (actual value) which, within the scope of the linearization and stability of the time base of the device corresponds to the preselected heating rate (theoretical value), and (ii) the true, instantaneous heating rate of the

sample which is in general not measurable and differs from the preselected heating rate. This true heating rate of the sample is additionally influenced by variations of the heat capacity and the thermal coupling of the sample.

The heating rate obtained from the experimental, measured pairs of $T(t),t$ values by differentiation with respect to t is a better approximation to the true heating rate of the sample than the preselected heating rate.

A3.3. Sample temperature lag

In a scanning calorimeter, the temperature of the furnace changes during measurement. Because the heat transport takes time, the sample temperature lags behind the furnace temperature. There is thus always a thermal lag between the controlled furnace temperature and the sample temperature. This difference increases with the heat flow rate due to the proportionality of heat flow rate and associated temperature gradient. The sample temperature lag therefore depends on the heat flow rate into the sample and, thus, on the heat capacity of the sample, its coupling and the heating or cooling rate.

Due to the relation between heat flow rate and heat capacity of the sample (Eq. (8)), an analogous formulation is valid for the difference between the measured apparent heat capacity and the true heat capacity of the sample (Fig. A8).

The true heat flow rate into the sample is calculated from the heat capacity C_{tr} as

$$\Phi_{tr}(T) = C_{tr}(T)\frac{dT_S}{dt} \tag{A6}$$

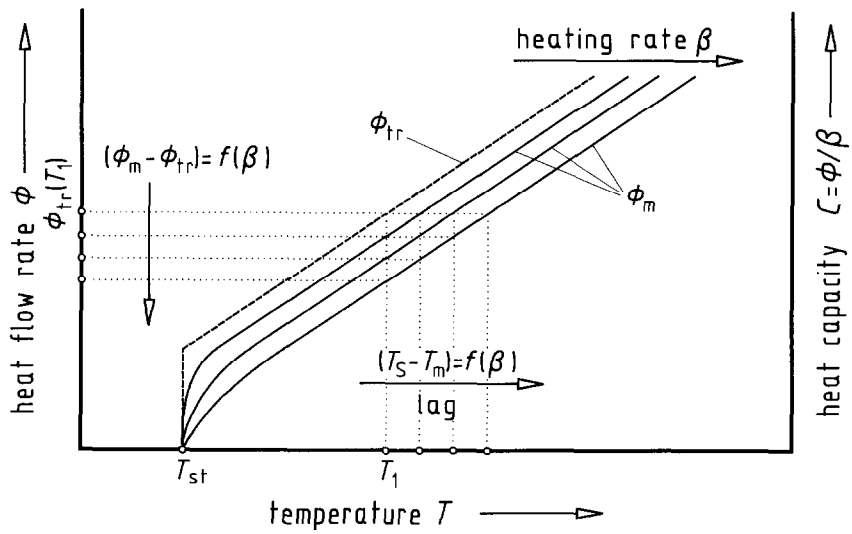

Fig. A8. Differences between true and measured heat flow rates in heat flow rate measurement. T program temperature; Φ, heat flow rate; C, heat capacity, T_{st}, starting temperature; β, heating rate; T_S, sample temperature; T_m, measured temperature; Φ_m, measured heat flow rate; Φ_{tr}, true sample heat flow rate [34].

where dT_S/dt is the actual, true sample heating rate. Because the sample temperature is lower than the temperature displayed, the heat flow displayed is also too low (compared with the true heat flow) due to the increase in C_{tr} with temperature which is generally monotonous away from phase transitions.

An additional difference between sample temperature and displayed temperature results from the temperature profile in thick samples. During the stationary heating at a constant heating rate, a parabolic temperature profile develops. The mean temperature of the sample is a function of its heat capacity C_p, its thermal conductivity λ, its density ρ, its thickness d and the heating rate β. For the difference between the temperature at the lower edge of the sample (point of contact with the base) and the mean sample temperature, the following is valid:

$$\Delta T = \frac{C_p \rho}{3\lambda} \beta d^2 \tag{A7}$$

This temperature difference must be added to the one mentioned above. It results in an additional lag of the measured heat flow rate compared with the true heat flow rate. If heat capacities are calculated from the measured heat flow rate curve (see Section 5.1.2), these are also systematically too low (see Fig. A8).

Because the temperature dependence of the heat capacity is normally not very strong, the effects discussed are not very important. For precision measurements ($< 1\%$), they should, however, be taken into account and, if necessary, allowed for computationally (deconvolution) [35].

A4. Important thermodynamic fundamentals

The isochoric mode of operation is very rare in scanning calorimetry; therefore the enthalpy H is the quantity of state suitable for description. In the general case, the enthalpy is a function of the temperature T, the pressure p and the variable reaction term ξ (when the physical or chemical composition of the sample varies). The total differential of $H(T,p,\xi)$ thus reads

$$dH = \left(\frac{\partial H}{\partial T}\right)_{p,\xi} dT + \left(\frac{\partial H}{\partial p}\right)_{T,\xi} dp + \left(\frac{\partial H}{\partial \xi}\right)_{T,p} d\xi \tag{A8}$$

Calorimetry means the measurement of heats Q_m or heat flow rates Φ_m. The relation between the quantities of enthalpy, heat and other forms of energy exchanged E_i is given by the first law of thermodynamics

$$\delta Q_m = \left(\frac{\partial H}{\partial T}\right)_{p,\xi} dT + \left[\left(\frac{\partial H}{\partial p}\right)_{T,\xi} - V\right] dp + \left(\frac{\partial H}{\partial \xi}\right)_{T,p} d\xi + \sum_i dE_i \tag{A9}$$

The measured heat δQ_m depends on the path. The quantity

$$\left(\frac{\partial H}{\partial T}\right)_{p,\xi} = C_{p,\xi}(T) \tag{A10}$$

designates the heat capacity at constant pressure and constant composition. The second term in Eq. (A9) is the heat effect when the pressure in the system varies

(with effect on the sample), and

$$\left(\frac{\partial H}{\partial \xi}\right)_{T,p} = \Delta H = \sum_i \nu_i H_i \tag{A11}$$

is the enthalpy variation related to the amount of substance and associated with a transformed fraction $\Delta\xi = 1$ mol at constant temperature and constant pressure (enthalpy of phase transition $\Delta_{trs}H$, enthalpy of mixing $\Delta_{mix}H$, reaction enthalpy $\Delta_r H$, wetting enthalpy $\Delta_\sigma H$ and others).

The last term in Eq. (A9) covers an exchange of other forms of energy with the system investigated (which is, however, rather rare in practice), e.g. mechanical energy (for example in the form of deformation effects on the sample or agitation energy), electrical energy, electromagnetic radiation.

When Eq. (A9) is used in practice, it is to be borne in mind that the enthalpy of a substance also depends on the surface/volume ratio. According to Kelvin, the smaller the radius of curvature of the surface of a body, the greater the chemical potential of this body. The result of this is a lower transition temperature and higher value of the enthalpy of transition of nanocrystalline or microcrystalline substances.

On condition that the last addend in Eq. (A9) is zero, the following equation is obtained for the heat flow rate under ideal conditions:

$$\frac{\delta Q_m}{dt} = \Phi_m = C_{p,\xi}(T)\frac{dT}{dt} + \left[\left(\frac{\partial H}{\partial p}\right)_{T,\xi} - V\right]\frac{dp}{dT}\frac{dT}{dt} + \left(\frac{\partial H}{\partial \xi}\right)_{T,p}\frac{d\xi}{dt} \tag{A12}$$

This equation also forms the basis of the kinetic evaluation of DSC curves.

The pressure dependence of the heat capacity C_p is so slight that a correction will not be necessary even if the acting pressure increases by several bar as in, for example, hermetically sealed crucibles heated to 600°C.

For the temperature dependence of the reaction enthalpy ΔH, the Kirchhoff equation obtained from Eq. (A11) by differentiation is valid.

$$\left(\frac{\partial \Delta H}{\partial T}\right)_{p,\xi} = \left(\frac{\partial C_{p,\xi}}{\partial \xi}\right)_{T,p} = \sum_i \left(\frac{\partial C_{p,\xi}}{\partial n_i}\right)_{T,p}\frac{dn_i}{d\xi} = \sum_i \nu_i C'_{p,i} \tag{A13}$$

where $C'_{p,i}$ are the partial heat capacities (related to the amount of substance) of the substances involved at constant pressure, ν_i are the stoichiometric numbers and n_i the amount of substance.

In the case of transitions of two coexisting phases (phase transitions), the heat capacities C_p of the phases involved are replaced by the equilibrium heat capacities C_{eq}. For evaporation or sublimation equilibria, these are the saturation heat capacities C_s. The relation between C_{eq} and C_p for each of the phases involved is

$$C_{eq} = C_p - \frac{\Delta_{trs}H}{\Delta_{trs}V}\left(\frac{\partial V}{\partial T}\right)_p \tag{A14}$$

In scanning calorimetry, the baseline below a peak is not accessible by experiment. For the computational determination of the baseline, Table A7 gives the heat capacities to be used for the various processes (see Annex A2).

Table A7
Heat capacities to be used for calculating baselines under a peak

Process	Heat capacity to be used
Phase transitions	Equilibrium or saturation heat capacities of the phases involved
Reactions between substances with ideal behaviour	Heat capacities of the pure substances involved
Reactions between substances with real behaviour, reactions in mixtures	Partial heat capacities for the initial and final concentrations of the substances involved

When peak areas are determined by means of the computer programs furnished by the manufacturer of the calorimeter, the graphic representation of the curve of measured values as a function of the measurement or program temperature frequently gives the impression that integration is carried out over the temperature. In fact, integration is carried out over the time, as there is no linear relation between temperature and time during a transition (see Annex A3).

It should, however, be pointed out that in practice many of the thermodynamic factors of influence are at present scarcely of significance in view of the uncertainty of measurement of the calorimeters.

A5. Difference between heat calibration factor and heat flow rate calibration factor

A scanning calorimeter serves to determine heat flow rates from measured temperature differences. Accordingly, there are always temperature differences between sample and reference sample during the measurement, and as a result, the heat exchange between sample and reference sample and the respective environment varies. However, because the radiation exchange increases nonlinearly with temperature, the overall heat exchange is also nonlinearly linked with the temperature difference between sample and reference sample. In the case of major temperature differences, the same applies to the heat exchange by convection. Consequently, the measured temperature difference (and thus the measured differential heat flow rate Φ_m) is nonlinearly linked with the true heat flow rate into the sample Φ_{tr}. This results in the calibration factor K_Φ in the (linearly formulated) Eq. (1) becoming a function of the differential heat flow rate Φ_m

$$\Phi_{tr} = K_\Phi(\Phi_m)\Phi_m \tag{A15}$$

Because the measured heat flow rate Φ_m depends on sample parameters (C_p,m) and on the heating rate, K_Φ also implicitly depends on these quantities. Furthermore, it follows from Fourier's law that K_Φ is in any case determined by the thermal conduction path and its properties (thermal conductivity, heat transfer paths). Because these quantities are always a function of temperature, K_Φ is always temperature dependent. This dependence is essentially associated with the instru-

ment properties and is thus basically invariable; in modern scanning calorimeters, it is automatically taken into consideration.

For heat calibration, Eq. (3), which is obtained from Eq. (1) by integration over the peak, is valid. If, however, K_Φ depends on Φ_m, this factor cannot be placed before the integral, and the following is obtained from Eq. (A15):

$$Q_{tr} = \int \Phi_{trs}\,dt = \int (\Phi_{tr} - \Phi_{bl})\,dt = \int [K_\Phi(\Phi_m)\Phi_m - K_\Phi(\Phi_{bl})\Phi_{bl}]\,dt \qquad (A16)$$

From a comparison with Eq. (3) it follows that K_Q is an integral mean value over the function $K_\Phi(\Phi_m)$ in the area of a peak. Because Φ_m can vary considerably during a peak, the difference between K_Φ and K_Q is normally significant (see Annex A1.2).

A6. Weighing regulation

The clean crucible to be used is first weighed as accurately as possible (microbalance). The required quantity of the calibration substance (if necessary pressed at low pressure to form a pellet) is exactly weighed into the crucible. In general, the crucible is then tightly sealed to prevent evaporation losses, reactions with the atmosphere and the like.

In the case of slightly volatile substances, it may become necessary to determine the mass of the sample from the difference between the mass of the filled, hermetically sealed crucible and the mass of the empty crucible. In this case, preliminary tests are to be carried out in order to determine whether mass losses result during the sealing process due to abrasion of crucible material; in this case, the measurements would be based on false quantities.

In general, reweighings are to be carried out after the measurement to determine whether the mass of the crucible and of the sample has changed as a result of reactions, evaporation or other effects. If this is the case, this must be taken into consideration when the errors are assessed.

For hygroscopic substances, weighed crucibles are to be used the cover of which is provided with a small hole. The substance is to be dehydrated in the calorimeter at a suitable temperature; its mass is determined by weighing after the measurement.

A7. *List of symbols*

a, b, c, d	coefficients for fitting polynomials
A	peak area
B	coefficient of regression of a fitted curve
c_m	measured specific heat capacity
$\bar{c}_m$	mean measured specific heat capacity
C_{eq}	equilibrium heat capacity
C_p	heat capacity at constant pressure
C'_p	partial heat capacity at constant pressure
C_R	heat capacity of the reference sample

C_S	heat capacity of the sample
C_{tr}	true heat capacity
d	sample thickness
E_{el}	electric energy
f	scale factor for the graphical determination of heat flow rates
f_L	correction factor for the power released in the supply lines
H	enthalpy
i	counting index
I	electric current
I_{cal}	calibration current
K	calibration factor
K_Φ	calibration factor for heat flow rate measurements
K_Q	calibration factor for heat measurements
$\bar{K}_Q$	mean calibration factor for heat measurements
m	mass
M	molar mass
p	pressure
P	electric power
Q	heat
Q_m	measured heat
$\bar{Q}_m$	mean measured heat
Q_{tr}	true sample heat
R	electrical resistance
R_w	supply line resistance
s^2	variance
S/N	signal-to-noise ratio
t	time
t_{end}	temperature program end time
t_f	final peak time
t_i	initial peak time
t_{st}	temperature program starting time
T	thermodynamic temperature
T_f	final peak temperature
T_i	initial peak temperature
T_m	measured temperature
T_{st}	starting temperature
T_R	reference sample temperature
T_S	sample temperature
T_{trs}	transition temperature
U	voltage
U_Φ	output voltage of a thermopile
V	volume
w	statistical weight for best-value determination
x_s	graphically read displayed sample heat flow rate
x_0	graphically read displayed zero line heat flow rate

β	heating rate
$\Delta\Phi_{SR}$	displayed heat flow rate with sample and reference sample
$\Delta\Phi_{tr}$	difference between true heat flow rates
Δt	heating time
ΔT	temperature difference
$\Delta_{trs}H$	enthalpy of transition
$\Delta_{trs}V$	transition volume variation
Δx	graphically determined sample and zero line heat flow rate difference
$\Delta x'$	graphically determined displacement-corrected heat flow rate
Δx_{iso}	graphically determined heat flow rate for displacement correction
λ	thermal conductivity
ν	stoichiometric number
Φ_0	zero line heat flow rate
Φ_{bl}	baseline heat flow rate
Φ'_0	displacement-corrected zero line heat flow rate
Φ_d	displayed heat flow rate
Φ'_d	displacement-corrected displayed heat flow rate
Φ_i	interpolated isothermal heat flow rate
$\Phi_{iso,end}$	isothermal end line
$\Phi_{iso,st}$	isothermal starting line
Φ_m	measured heat flow rate
$\Phi_{R,tr}$	true heat flow rate into the reference sample
$\Phi_{S,tr}$	true heat flow rate into the sample
Φ_S	displayed heat flow rate with sample
$\Phi_{S,cal}$	displayed heat flow rate with calibration sample
Φ_{tr}	true sample heat flow rate
Φ_{trs}	transition heat flow rate
Φ_w	heat flow rate released in supply lines
σ_{n-1}	standard deviation
ρ	density
τ	time constant of the measuring system
θ	temperature in °C
$\bar{\theta}$	mean temperature in °C
ξ	variable reaction term

References

[1] John O. Hill (Ed.), For Better Thermal Analysis, 3rd edn., International Confederation for Thermal Analysis (ICTA), 1991.

[2] Quantities, Units and Symbols in Physical Chemistry, 2nd edn., International Union of Pure and Applied Chemistry (IUPAC), Blackwell, Oxford, 1993.

[3] G.W.H. Höhne, H.K. Cammenga, W. Eysel, E. Gmelin and W. Hemminger, Die Temperaturkalibrierung dynamischer Kalorimeter, PTB-Mitt., 100 (1990) 25–31; The temperature calibration of scanning calorimeters, Thermochim. Acta, 160 (1990)1–12.

[4] H.K. Cammenga, W. Eysel, E. Gmelin, W. Hemminger, G.W.H. Höhne and S.M. Sarge, Die Temperaturaturkalibrierung dynamischer Kalorimeter II. Kalibriersubstanzen, PTB-Mitt., 102

(1992) 13–18; The temperature calibration of scanning calorimeters. Part 2. Calibration substances, Thermochim. Acta, 219 (1993) 333–342.

[5] D.A. Ditmars, S. Ishihara, S.S. Chang, G. Bernstein and E.D. West, Enthalpy and heat-capacity standard reference material. Synthetic sapphire (α-Al_2O_3) from 10 to 2250 K, J. Res. Natl. Bur. Stand., 87 (1982) 159–163.

[6] D.L. Martin, "Tray" type calorimeter for the 15–300 K temperature range: copper as a specific heat standard in this range, Rev. Sci. Instrum., 58 (1987) 639–646.

[7] G.J. Szasz, J.A. Morrison, E.L. Pace and J.G. Aston, Thermal properties of cyclopentane and its use as a standard substance in low temperature thermal measurements, J. Chem. Phys., 15 (1947) 562–564; $\overline{\Delta_{trs}H(122\ K)} = 1166.6$ cal mol^{-1}, $\overline{\Delta_{trs}H(138\ K)} = 82.34$ cal mol^{-1}, $\Delta_{fus}H = 144.63$ cal mol^{-1}, 1 cal = 4.1833 J_{int}, 1 J_{int} = 1.00019 J, $M = 70.13$ g mol^{-1}.

[8] G.B. Adams, Jr., H.L. Johnston and E.C. Kerr, The heat capacity of gallium from 15 to 320°K. The heat of fusion at the melting point, J. Am. Chem. Soc., 74 (1952) 4784–4787; $\Delta_{fus}H = 1335$ cal mol^{-1}, 1 cal = 4.184 J, $M = 69.72$ g mol^{-1}, statistical weight w for best-value determination: $w = 1$.

[9] E.B. Amitin, Yu.F. Minenkov, O.A. Nabutovskaya, I.E. Paukov and S.I. Sokolova, Thermodynamic properties of gallium from 5 to 320 K, J. Chem. Thermodyn., 16 (1984) 431–436; $\Delta_{fus}H = 5551.8$ J mol^{-1}, $M = 69.723$ g mol^{-1}, $w = 1$.

[10] F. Grønvold, Heat capacity of indium from 300 to 1000 K. Enthalpy of fusion, J. Therm. Anal., 13 (1978) 419–428; $\Delta_{fus}H = 3283$ J mol^{-1}, $M = 114.82$ g mol^{-1}, $w = 3$.

[11] K.H. Schönborn, W. Hemminger and J. Reichelt, Determination of the enthalpy of fusion of indium by direct comparison with Joule heats, Thermochim. Acta, 69 (1983) 127–136; $\Delta_{fus}H = 28.65$ J g^{-1}, $w = 2$.

[12] J. Ancsin, Melting curves and heat of fusion of indium, Metrologia, 21 (1985) 7–9; $\Delta_{fus}H = 28.53$ J g^{-1}, $w = 3$.

[13] W. Hemminger and K. Raetz, Bestimmung der Schmelzwärme von Zinn und von Indium mit einem Dynamischen Wärmestrom-Differenzkalorimeter, PTB-Mitt., 99 (1989) 83–88; a check of the corrections yielded $\Delta_{fus}H(In) = 28.64$ J g^{-1} and $\Delta_{fus}H(Sn) = 60.24$ J g^{-1}, $w = 2$.

[14] F. Grønvold, Enthalpy of fusion and temperature of fusion of indium and redetermination of the enthalpy of fusion of tin, J. Chem. Thermodyn., 25 (1993) 1133–1144; $\Delta_{fus}H(In) = 3296$ J mol^{-1}, $M = 114.818$ g mol^{-1}, $\Delta_{fus}H(Sn) = 7179$ J mol^{-1}, $M = 118.710$ g mol^{-1}, $w = 3$.

[15] F. Grønvold, Heat capacity and thermodynamic properties of metallic tin in the range 300 to 1000 K. Fusion characteristics, Rev. Chim. Miner., 11 (1974) 568–584; $\Delta_{fus}H = 7195$ J mol^{-1}, $M = 118.69$ g mol^{-1}, $w = 3$.

[16] D.A. Ditmars, J. Chem. Thermodyn., to be published; (National Institute of Standards and Technology, Certificate of Analysis, Standard Reference Material 2220, Temperature and enthalpy of fusion–tin, May 16, 1989); $\Delta_{fus}H = 7147$ J mol^{-1}, $M = 118.69$ g mol^{-1}, $w = 3$.

[17] F. Grønvold, Heat capacity and thermodynamic properties of bismuth in the range 300 to 950 K. Fusion characteristics, Acta Chem. Scand. Ser. A, 29 (1975) 945–955; $\Delta_{fus}H = 11131$ J mol^{-1}, $M = 208.98$ g mol^{-1}, $w = 3$.

[18] K. Raetz, Determination of the heat of fusion of bismuth with a heat-flux DSC, Thermochim. Acta, 151 (1989) 323–331; a check of the corrections yielded $\Delta_{fus}H = 53.03$ J g^{-1}, $w = 2$.

[19] M. Kano, Adiabatic calorimeter for the purpose of calorimetry in the solid, liquid and supercooled phases of metals, J. Phys. E: Sci. Instrum., 22 (1989) 907–912; $\Delta_{fus}H = 11478$ J mol^{-1}, $M = 208.98037$ g mol^{-1}, $w = 3$.

[20] L. Deniélou, Y. Fournier, J.-P. Petitet and C. Téqui, Étude calorimétrique des sels entre 273°K et 1533°K. Technique et application aux sulfates alcalins, Rev. Int. Hautes Temp. Réfract., 8 (1971) 119–126; $\Delta_{trs}H = 6110$ cal mol^{-1}, $M = 109.94$ g mol^{-1}, 1 cal = 4.184 J, $w = 2$.

[21] R.P. Clark, Thermal data for lithium sulfate and binary eutectics lithium sulfate–lithium chloride, lithium sulfate–sodium chloride, and lithium sulfate–potassium chloride, J. Chem. Eng. Data, 20 (1975) 17–19: $\Delta_{trs}H = 5.98$ kcal mol^{-1}, $M = 109.94$ g mol^{-1}, 1 cal = 4.184 J, $w = 2$.

[22] K.-H. Breuer and W. Eysel, The calorimetric calibration of differential scanning calorimetry cells, Thermochim. Acta, 57 (1982) 317–329; $\Delta_{trs}H = 24.46$ kJ mol^{-1}, $M = 109.94$ g mol^{-1}, $w = 1$.

[23] W. Eysel and K.-H. Breuer, Differential scanning calorimetry: simultaneous temperature and calorimetric calibration, in J.F. Johnson and P.S. Gill (Eds.), Analytical Calorimetry, Vol. 5, Plenum, New York, 1984, pp. 67–80; $\Delta_{trs}H = 25.02$ kJ mol^{-1}, $M = 109.94$ g mol^{-1}, $w = 1$.

[24] G.W.H. Höhne, W. Eysel and K.-H. Breuer, Results of a round robin experiment on the calibration of differential scanning calorimeters, Thermochim. Acta, 94 (1985) 199–204; $\Delta_{trs}H = 24.65$ kJ mol^{-1}, $M = 109.94$ g mol^{-1}, $w = 1$.

[25] J. Nölting and V. Freystein, personal communication 1993; $\Delta_{trs}H = 255.6$ J g^{-1}, $w = 3$. We thank J. Nölting and V. Freystein for determining this value.

[26] M. Tischler, High-accuracy thermal analysis of the solid–solid phase transition of lithium sulfate powders, Thermochim. Acta, 231 (1994) 87–108; $\Delta_{trs}H = 26.1$ kJ mol^{-1}, $M = 109.9456$ g mol^{-1}, $w = 1$.

[27] R.A. McDonald, Enthalpy, heat capacity, and heat of fusion of aluminum from 366° to 1647°K, J. Chem. Eng. Data, 12 (1967) 115–118; $\Delta_{fus}H = 2560$ cal mol^{-1}, 1 cal = 4.184 J, $M = 26.98$ g mol^{-1}, $w = 2$.

[28] U. Schmidt, O. Vollmer and R. Kohlhaas, Thermodynamische Analyse kalorimetrischer Messungen an Aluminium und Wolfram im Bereich hoher Temperaturen, Z. Naturforsch. Teil A, 25 (1970) 1258–1264; $\Delta_{fus}H = 10700$ J mol^{-1}, $M = 26.98$ g mol^{-1}, $w = 3$.

[29] L. Malaspina, R. Gigli and G. Bardi, Determinazione di alcuni parametri termodinamici mediante un micro-calorimetro calvet per alte temperature, Calore, 42 (1971) 317–326; $\Delta_{fus}H = 2610$ cal mol^{-1}, 1 cal = 4.186 J, $M = 26.98$ g mol^{-1}, $w = 1$.

[30] W.F. Hemminger and S.M. Sarge, The baseline construction and its influence on the measurement of heat with differential scanning calorimeters, J. Therm. Anal., 37 (1991) 1455–1477.

[31] A.P. Gray, Polymer crystallinity determinations by DSC, Thermochim. Acta, 1 (1970) 563–579.

[32] S.C. Mraw and D.F. Naas, The measurement of accurate heat capacities by differential scanning calorimetry. Comparison of d.s.c. results on pyrite (100 to 800 K) with literature values from precision adiabatic calorimetry, J. Chem. Thermodyn., 11 (1979) 567–584.

[33] E. Hanitzsch, Modification of the conventional measuring method to determine the specific heat capacity using a Perkin-Elmer DSC 2, Thermochim. Acta, 187 (1991) 275–281.

[34] M.J. Richardson, The application of differential scanning calorimetry to the measurement of specific heat, in K.D. Maglić, A. Cezairliyan and V.E. Peletsky (Eds.), Compendium of Thermophysical Property Measurement Methods, Vol. 2, Recommended Measurement Techniques and Practices, Plenum, New York, 1992, pp. 519–545.

[35] G.W.H. Höhne and J.E.K. Schawe, Dynamic behaviour of power compensated differential scanning calorimeters. Part 1. DSC as a linear system, Thermochim. Acta, 229 (1993) 27–36.